# SCREENING MEASUREMENT OF INDOOR RADON-222 CONCENTRATIONS BY GAMMA-RAY SPECTROMETRY IN KENYATTA UNIVERSITY

**By**

**Margaret Wairimu Chege (B.Ed (Sc))**
**Reg. No. I56/5995/03**
**Physics Department**

**A thesis submitted in partial fulfillment of the requirement for the award of the degree of Master of Science in the School of Pure and Applied Sciences of Kenyatta University**

**2007**

**DECLARATION**

This thesis is my original work and has not been presented for a degree in any other university.

Margaret Wairimu Chege
(I56/5995/03)
Department of Physics
Kenyatta University
P. O. Box43844
Nairobi, Kenya.

Signature..... Date 06/03/07

This thesis has been submitted for examination with the approval of my university supervisors:

Prof. I. V. S. Rathore

Physics Department
Kenyatta University
P. O. Box 43844
Nairobi.

Signature ..... Date 03/03/07

Prof. S. C. Chhabra

Chemistry Department
Kenyatta University
P. O. Box 43844
Nairobi.

Signature ..... Date 3/3/07

Dr. A. O. Mustapha

Physics Department
University of Nairobi
P. O. Box 30197
Nairobi

Signature ..... Date 02-03-07

## DEDICATION

This thesis is dedicated to my sisters
Wanjiru, Wambui, Njeri and Wanjiku

**ACKNOWLEDGEMENTS**

I wish to express my gratitude to my thesis supervisors, Prof. I. V. S. Rathore, Prof. S. C. Chhabra and Dr. A. O. Mustapha for their guidance and useful suggestions throughout the course of research, and for the many fruitful discussions on radiation environment in dwellings. I sincerely acknowledge the support from Mr. Maina, the Director, Institute of Nuclear Science, University of Nairobi, for the research facilities provided in this study. My gratitude also goes to the staff and students in the Physics Department, Kenyatta University and the Institute of Nuclear Science, University of Nairobi for the friendly atmosphere during the research period. Thanks are also due to Mr. Njuguna, the Chief Technician, Physics Department, Kenyatta University for his assistance during the research period and presentation. I acknowledge the assistance from Geography Department, Kenyatta University for providing the meteorological data, and to the Chemistry Department, for allowing the use of their facilities. My appreciation goes to the Department of Cultural Studies and the managers of the Culture Village, Kenyatta University, for allowing the use of the model traditional huts for this research.

**ABSTRACT**

Rn-222 and its progeny are the largest contributors to the total effective dose received by the general public. It is therefore of great concern to monitor radon concentration in dwellings. Measurements of indoor $^{222}Rn$ concentrations in modern and traditional buildings were carried out for comparison purposes. The measurements were carried out in the Kenyatta University campus in Nairobi, Kenya, where modern buildings and a number of model traditional buildings co-exit. Charcoal canisters were employed to sample $^{222}Rn$ by exposing the activated canisters at the sampling sites for 48 hours. After exposure, gamma emissions from $^{222}Rn$ daughters trapped in the canister were analysed using NaI(Tl) detector, and the $^{222}Rn$ concentrations at the sampling sites were calculated. The average $^{222}Rn$ concentration during the sampling period was 188 $Bq/m^3$. $^{222}Rn$ concentration varied from 30.2 to 315.4 $Bq/m^3$ in the traditional houses and from 115.76 to 257.2 $Bq/m^3$ in modern buildings. The average $^{222}Rn$ concentration was higher in the modern building than in the traditional ones. The contribution of building materials as sources of indoor $^{222}Rn$ was also investigated. This involved gamma spectrometric analysis of samples of building materials to determine their $^{226}Ra$ concentration, using HPGe detector. The activity concentration of $^{226}Ra$ ranged from 11.66-101.93 $Bq/m^3$ with the highest value found in the mud used in the construction of the model traditional houses. The ranges of $^{40}K$ and $^{232}Th$ in the samples are 254.46-1246.79 $Bq/m^3$ and 15.3 to 148.34 $Bq/m^3$, respectively. The bulk exhalation rates of $^{222}Rn$ from selected building materials were evaluated by enclosing samples in a $^{222}Rn$ free can and monitoring $^{222}Rn$ accumulation with time. $^{222}Rn$ exhalation rate was highest in the mud samples and lowest in stone and concrete samples.

## LIST OF TABLES

## LIST OF FIGURES

## LIST OF ABBREVIATIONS

| | |
|---|---|
| ADC | Analog-to-Digital Converter |
| Amp | Amplifier |
| BEIR | Biological Effects of Ionising Radiation |
| DNA | Deoxyribonucleic Acid |
| EPA | Environmental Protection Agency |
| FWHM | Full Width at Half Maximum |
| GANAAS | Gamma Spectrum Analysis Activity Calculations and Neutron Activation Analysis Software |
| HPGe | High Purity Germanium Detector |
| HV | High Voltage |
| IAEA | International Atomic Energy Agency |
| ICRP | International Commission on Radiological Protection |
| MCA | Multi-Channel Analyser |
| NaI(Tl) | Sodium Iodide Thallium Activated Detector |
| PMT | Photomultiplier Tube |
| Preamp | Preamplifier |
| UNSCEAR | United Nations Scientific Committee on Effects of Atomic Radiation |
| WHO | World Health Organization |

## TABLE OF CONTETS

# CHAPTER 1

# INTRODUCTION

## 1.1 BACKGROUND TO THE STUDY

Public awareness of exposures to ionizing radiation has focused primarily on nuclear power generation of electrical energy. However, more recently there has been increased concern about exposures associated with the enhanced natural radiation environment. Natural radioactivity is composed of the cosmogenic and primordial radionuclides. Cosmogenic radionuclides, such as $^{3}H$, $^{7}Be$, $^{14}C$, and $^{22}Na$, are produced by the interaction of cosmic-ray particles (mainly high-energetic protons) in the earth's atmosphere. Primordial radionuclides are left over from when the world and the universe were created. They are typically long lived, with half-lives often on the order of hundreds of millions of years.

Only those radionuclides with half-lives comparable to the age of the earth, and their decay products, can still be found on the earth's crust today, e.g. $^{40}K$, and the radionuclides from $^{238}U$and $^{232}Th$ series. The distribution of these naturally occurring radionuclides depends on the distribution of rocks from which they originate and the process which concentrate them (Mohanty *et al.*, 2003). They are ubiquitous in the environment hence they are the main source of radiation exposure to the general population. Approximately 90% of the total annual radiation dose received by the general public is derived from these natural sources and the single largest component of this dose is that due to radon and its decay products in the indoor environment. $^{222}Rn$ gas is

responsible for over 50% of the total annual radiation exposure to the general public (UNSCEAR, 2000).

Radon has been recognized as a health risk for a long time. The first indications that radon and radon daughter products could constitute a risk to human health came in the 1920s. As an increased mortality due to lung cancer among mineworkers who were exposed to mine air with radon concentrations of tens of thousands to millions of $Bq/m^3$ was observed, the connection between radon and lung cancer was established (BEIR IV, 1988).

$^{222}Rn$ (commonly referred to as radon) is an alpha emitter with a half-life of about 3.82 days that decays to a short-lived series of daughters (Table 1.1).

**Table 1.1: $^{222}Rn$ Decay Series (Dumont *et al.*, 1988)**

| | Decay by-product | Half-life |
|---|---|---|
| $^{222}Rn$ | Alpha particle | 3.82 days |
| $^{218}Po$ | Alpha particle | 3.05 min |
| $^{214}Pb$ | Beta particle and gamma radiation | 26.8 min |
| $^{214}Bi$ | Beta particle and gamma radiation | 19.7 min |
| $^{214}Po$ | Alpha particle | 0.000003 min |

Unlike radon, the daughters are charged solids and form into small molecular clusters or attach to aerosols in the air after their formation. Most of these daughters have half-lives

of less than 30 minutes as indicated in Table 1.1. When they are inhaled, the particulate daughters may be deposited in the lung on the respiratory epithelium; radon by contrast is largely exhaled, although some radon is absorbed through the lung.

Radon itself is not responsible for the critical dose of radioactivity delivered to the lung that causes cancer. Rather the alpha particles from the radon daughters are responsible, most notably $^{218}Po$ and $^{214}Po$. When they are inhaled, these radon daughter particles are not dispersed throughout the body, but accumulate in the lungs and tracheobronchial tree, particularly in bifurcations. Since the alpha particles cannot penetrate more than a fraction of a millimeter into the lung tissue before smashing into an atom, the damage is concentrated on the cells in the immediate area. The alpha decays of the two radioisotopes in the decay chain deliver the energy to target cells in the respiratory epithelium that is considered to cause radon-associated lung cancer (Bailey, 1994; European Commission, 1998).

## 1.2 RADON IN DWELLINGS

The connection between radon and lung cancer among mineworkers has raised concern that radon in homes might be causing lung cancer in the general population, although the radon levels in most homes are much lower than in most mines. It is also well known that peoples living habits do influence their exposures to radon considerably (Hirning, 1992; Conkwright and Gast, 2005). For instance, people who work in indoor environments are likely to be more exposed than those who work outdoor. Also building designs and the

type of building materials are some of the other influential factors. Therefore exposures to radon can be quite variable.

Though the main source of radon in the air is subsoil significant radon concentrations have been found in dwellings situated in areas of low geological radon exhalation from the soil (Nero *et al.,* 1984). Clearly, radon is also affected by the other factors mentioned as well as ventilation and meteorological variables like precipitation and temperature (Orlando *et al.*, 2004).

***Living Habits in Kenya***

Kenya is a tropical country. It has a rich culture from the different ethnic communities that live therein, like the Maasai, Kikuyu, Luyha and Luo. Most of these communities still uphold some of their traditional ways of life.

The biggest fraction of Kenyan population lives in the rural areas where traditional huts are constructed alongside modern buildings. A typical traditional hut in Kenya is constructed using cheap, locally available materials. Basically, soil (in some communities cow dung is added) is mixed with water to form relatively soft mud, which is then used to construct the walls of the hut. The floor is often bare. In some communities like the Maasai, the mud wall is extended to form the roof. In most communities though, either the huts are grass-thatched or roofed using iron sheets. These huts are often small in size with 2-4 small rooms. The room partitioning is done using either sticks or mud walls. The doors and windows are made from wood and often remain shut. On the other hand, the

modern buildings design is similar to those in other areas in the world; bungalows constructed from concrete blocks or natural stone.

This study was undertaken mainly at the Kenyatta University Campus, which has modern buildings and a cultural village with model traditional dwellings and partly at the Chiromo Campus of the University of Nairobi. It is envisaged that this study will give some insight on the relationship between building construction design and indoor radon concentration.

## 1.3 STATEMENT OF THE RESEARCH PROBLEM

Representative data and information on the status of environmental radon concentrations are inadequate in many parts of the world including Kenya. This shortcoming makes it difficult to arrive at global average values of some relevant environmental parameters, such as the action levels, etc. (UNSCEAR, 1988; Iyengar, 1990). Research in this line is therefore required in Kenya to provide information and representative data for the relevant environmental and health authorities, as well as create awareness among the general public about the typical levels of radon in the environment. It is also very important to conduct researches that will indicate how atmospheric parameters and the peoples living habits are influencing their levels of exposures to radon.

## 1.4 OBJECTIVES OF THE RESEARCH PROJECT

The principal aim of the research project is to provide information and generate database on indoor radon concentrations.

Specific objectives of the research project are:

I. To determine the concentrations of $^{222}Rn$ in indoor air in selected buildings and model traditional huts in Kenyatta University

II. Measure the concentrations of naturally occurring radionuclides in selected building materials (e.g. building stone and mud) and investigate the relationship between $^{226}Ra$ concentrations in the building material samples and the concentrations of $^{222}Rn$ in air analysed.

## 1.5 RATIONALE OF THE RESEARCH PROJECT

Investigations on natural radiation (especially indoor radon concentration) have received particular attention worldwide and led to intensive surveys in many countries. This subject has not received enough attention in Kenya although a few studies on natural radioactivity and indoor radon concentration measurements have been reported (Mustapha, 1999; Hashim, 2001; Maina *et al.*, 2004). Some of the benefits derivable from this study include:

i. An understanding of housing designs and their impact on the indoor radon concentrations (if any).

ii. Knowledge of the relationship between radon concentrations and climatic variables.

iii. An understanding of the seasonal variation in radon concentrations.

iv. Generation of information and data required for evaluating radiation exposure levels associated with radon and other naturally occurring radionuclides.

v. To make recommendations and suggestions about the need for regulation and control of indoor radon.

vi. Data obtained can be used to develop a model that can then be used to estimate radon levels in other parts of the country.

# CHAPTER 2

# LITERATURE REVIEW

## 2.1 THE HISTORY OF RADON

In 1899, while trying to measure the radiation that was emitted from radium, Pierre and Marie Curie observed an interesting phenomenon. The radioactive gas emitted from radium remained reactive for almost a month. In 1900, the German physicist Friedrich Ernst Dorn confirmed their finding by using a more active radium compound. Dorn called the highly radioactive gas a "radium emanation". The name was derived from the Latin word "emanare" – to elapse and "emanatio" – expiration. In 1908, the radium emanation was renamed niton from the Latin word "nitens", which means shining. In 1923, the International Committee for Chemical Elements and the International Union of Pure and Applied Chemistry chose the name radon, which was submitted by Gerhard Schmidt and Benjamin Adams to identify the colorless, odourless, tasteless, nonmetallic, nonflammable, inert, radioactive noble gas derived from radium (LaFavore, 1987).

Radon occurs as three different isotopes in nature, $^{219}Rn$, $^{220}Rn$ and $^{222}Rn$, one from each of the three natural radioactive decay series summarized in Table 2.1. $^{222}Rn$ (commonly referred to as radon (and is referred to as such in this thesis)) is formed through α-decay of $^{226}Ra$ in the decay chain of $^{238}U$ (Appendix B1). $^{220}Rn$, called thoron, is formed in the decay chain of $^{232}Th$ (Appendix B2). $^{222}Rn$ is considered to be the most important isotope as a radiological risk factor, because of its half-life of 3.82 days, which is a much longer time than 55.6 and 4.0 seconds that is the half-life for $^{220}Rn$ and $^{219}Rn$, respectively. Therefore $^{222}Rn$ has the ability to move a considerable distance before it decays. Thoron

mostly results in low levels indoors (UNSCEAR, 1993). Recent measurements in some countries have shown, however, that in certain situations the doses from thoron and its progeny are significant and comparable to those from radon (Sciocchetti, 1992; Doi, 1994).

**Table 2.1: The $^{238}U$, $^{232}Th$ and $^{235}U$ Series (Olsson and Tengstrom, 2004)**

| Series name | Mother Nucleus | Half-life | Stable Final Daughter Nucleus | Gas Half-life ($T_{1/2}$) |
|---|---|---|---|---|
| Thorium | $^{232}Th$ | $1.4 \times 10^{10}$ years | $^{208}Pb$ | $^{220}Rn$ (55.6 s) thoron |
| Uranium | $^{238}U$ | $4.5 \times 10^{9}$ years | $^{206}Pb$ | $^{222}Rn$ (3.82 days) radon |
| Actinium | $^{235}U$ | $7.1 \times 10^{8}$ years | $^{207}Pb$ | $^{219}Rn$ (4.0 s) actinon |

Radon can be condensed to a transparent liquid and to an opaque, glowing solid. Radon has a melting point of –71°C and a boiling point of –62°C. The gas has a density of 9.73 grams per liter at 0°C at one atmosphere, which makes it the densest gas known. Radon is undetectable to human senses and can only be detected and measured through the use of radon specific testing devices. The concentration in the air is measured in units of pCi/L or $Bq/m^3$. One Becquerel corresponds to one disintegration per second (1 dps). One pCi/L is equivalent to 37 $Bq/m^3$.

Radon has been used for several beneficial purposes. It has been used in (radon) therapy, in particular for the treatment of painful inflammatory and degenerative joint and spine diseases (Becker, 2004), and in radiography as a pre-determinant for both earthquakes and volcanic activity (Garcia *et al.*, 2000; Planinić *et al.*, 2001). Radon has also been

extensively used for uranium exploration (EPA, 1990c) and other radioactive ore bodies (Sengupta *et al.*, 2001). It is also useful in analysis of regional transport and for verifying the calculation condition of an atmospheric transport model for air pollutants on a regional scale (Sakashita *et al.*, 2004). It has been used in studies on geological processes like faulting and deformation (Sengupta *et al.*, 2005). Radon is, however, a class 'A' known human carcinogen and the second leading cause of lung cancer; the number one cause is cigarette smoking (Viera, 2000).

## 2.2 SOURCES OF RADON

There are four contributors to indoor radon concentrations in the home. These are: soil gas, emanation from building materials and diffusion through foundation, airflow and water. This is illustrated in Figure 2.1. UNSCEAR has made a very simple model to estimate the relative contribution of these sources: for a "typical" house with a radon concentration of 50 $Bq/m^3$ at ground floor, the contribution of soil, building materials and outdoor air are, ~60%, ~20 and ~20%, while for the upper floors in high rise buildings, where the radon concentration is estimated to be typically 20 $Bq/m^3$, these values became ~0%, ~50% and ~50% (UNSCEAR, 1993).

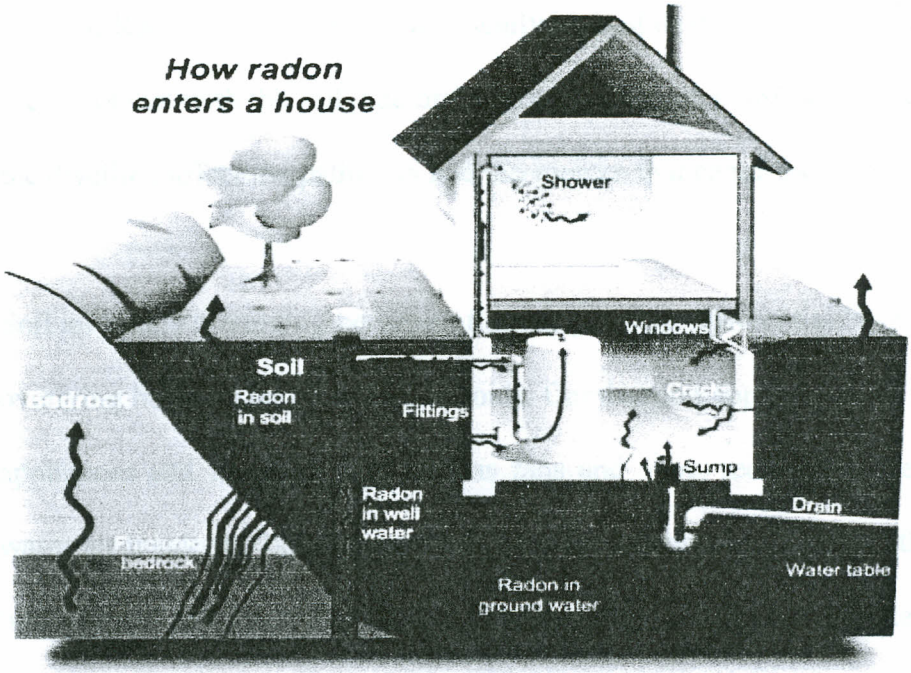


**Figure 2.1: How radon enters a house**

### 2.2.1. Soil

The largest fraction of radon concentration in indoor air is contributed from soil gas entry into the home (Greene, 2000; UNSCEAR, 1993). Radium, which is considered the direct parent compound of radon, is present in the majority of soils and rock formations. The radium concentration in the soil usually lies in the range 10 Bq/kg to 50 Bq/kg, but it can reach values of hundreds of Bq/kg (UNSCEAR, 1993).

When $^{226}Ra$ in the soil decays, some radon atoms are released from the solid matrix of the material. For a radon atom to escape from the mineral grain into the pore space, the decay must occur within the recoil distance of the grain surface. Movement of radon gas through soil is controlled by soil porosity (the percentage of air space in soil), permeability (the ease with which air or fluid can move through soil), and soil moisture

content. Radon concentrations are usually highest in the basements and ground floors that are in contact with the soil. Factors such as the design, construction, and the ventilation of the dwelling affect the pathways and the sources that can draw radon indoors.

Soil air enters a building because of an air pressure differential between the soil and the overlying building and foundation voids. Combustion appliances like furnaces, hot water appliances and fire places as well as fans and vents reduce the pressure indoors. The warm air inside the building moves upwards like inside a stark and this effect known as 'stark effect' reduces the inside air pressure. When the ground is frozen or soaked by rain the 'bottled up' radon in the ground moves to the warm permeable and disturbed ground underneath the house. The resulting pressure driven flow (advection) draws in radon through the openings or cracks and through the pores in the concrete.

Radon is also pulled in by the difference in radon concentration indoors and in the soil (diffusion). Radon tries to equalize the indoor concentration, and its atoms easily penetrate through the pores in the concrete or directly from dirt floors. Building foundations are rarely airtight hence radon-enriched soil air can enter a building through cracks in the foundation, utility pipes, wires and cables, or direct from dirt floor.

### 2.2.2. Building Materials

Radium presence in building materials causes exposure to persons living in dwellings - either by inhalation of radon daughters that are released from the building material to indoor air, or by gamma radiation that releases from the building material as a

consequence of the radioactive decay of the natural radionuclides present. Building materials are generally the second source of radon indoors, although in the 1970s they were considered the principle ones. Typical excess indoor radon concentration due to building materials is about 10–20 $Bq/m^3$, though in rare cases it may rise up to levels greater than 1000 $Bq/m^3$ (UNSCEAR, 1977).

The radon generation depends on the radium content, the age of the building material, the relative humidity and the sort and the amount of building material. However, the amount of generated radon can differ by an order of magnitude between similar building material samples (Michel, 2003). The activity concentration of radium in building materials may be high if the raw materials were taken from locations with high levels of natural radioactivity.

The transport of the generated radon gas depends on the porosity of the building materials. Mud and concrete used in construction cures by reacting with water (hydration). But almost half of the water added to the concrete and mud mixes for workability is surplus and has to evaporate. As the surplus water evaporates, it leaves a network of capillaries (pores).

For the concrete, the pores constitute 12 to 18% by volume. Their diameter is smaller than a human hair but much larger than radon atoms or water molecules. In the case of mud, the pores constitute about 50% and their diameter is far much larger than that of

concrete. These pore spaces allow easy movement of generated radon, hence elevated exhalation rate.

### 2.2.3. Water

In wells drilled in rock, the radon concentration of water may be high. When such water is used in household, radon will be partially released into the indoor air, causing an increase in the average radon concentration. In a few regions such as Finland and Maine (USA), tap water from wells drilled in rock has shown to contribute significantly to radon concentrations indoors (Dumont and Figley, 1988).

Radon concentrations in tap water from deep wells can range from 100 $kBq/m^3$ to 100 $MBq/m^3$ (UNSCEAR, 1988). The indoor radon concentration in these regions may be already high due to high entry rates of radon from the ground. The world average radon concentration in all types of water supplies is assumed to be 10 $Bq/m^3$ (UNSCEAR, 1993).

### 2.2.4. Outdoor Air

Outdoor air usually acts as a diluting factor due to its normally low radon concentration, but in some cases, as in high rise apartments built with materials having very low radium content, it can act as a real source. Until a few years ago the average radon gas concentration in the atmosphere at ground level was assumed to be of the order of a few $Bq/m^3$ e.g. in the range of 4 to 15 $Bq/m^3$ (Gesell, 1983), but more recent measurements indicate higher values, reaching some tens $Bq/m^3$ (Price *et al.*, 1994). Quite high

concentrations in the outdoor air have been reported near substantial radon sources, such as mine tailings or in the case of particular weather conditions such as thermal inversion or very low precipitation (Tyson *et al.*, 1993).

## 2.3 HEALTH IMPLICATIONS OF RADON

The story of radon as a source of lung cancer is a long one with historical accounts documenting a fatal lung cancer centuries ago in miners working in the Erz Mountains of Eastern Europe (Samet *et al.*, 2000). Over a century ago, the miners were found to have thoracic malignancy, later identified as primary cancer. By early $20^{th}$ century, levels of radon in the mines in this region were measured and found to be quite high; the hypothesis was soon advanced that radon was the cause of the unusually high rates of lung cancer.

Although not uniformly accepted initially, the findings of epidemiological studies of underground miners have given substantial evidence showing radon as a possible cause of lung cancer. The miners' cancer mortality rate was found five times the rate expected for the general population (BEIR IV, 1988)

It has also been scientifically proven that intracellular DNA can be damaged as a result of contact with an alpha particle, as with those involved in radon's radioactive decay sequence (Krewski *et al.,* 1999). Even allowing for a substantial degree of repair, the passage of a single alpha particle has the potential to trigger cancerous growth of cells

which it does not kill outright. Since these effects take place in a random manner at the cellular level, there is no such thing as a "harmless" dose.

In 1999, the National Research Council of the National Academy of Sciences published the BEIR VI report, which assessed the risks to the USA population from radon in homes. The authors of this study, sponsored by the EPA, had the benefit of extensive new information not available to the authors of the Academy's previous BEIR IV report on the risks from radon and other alpha emitters. On the basis of epidemiologic evidence from miners and an understanding of the biological effects of alpha radiation, the committee concluded that residential exposure to radon is expected to be a cause of lung cancer in the population.

Based on a statistical analysis of epidemiological data on 11 cohorts of occupationally exposed underground miners, the committee developed two preferred risk models from which they projected, respectively, 15,400 or 21,800 excess lung cancer cases in the USA each year. An analysis of the uncertainties suggested a range of 3,000 to 33,000 cases per year. The committee concluded that there existed a public health problem and that indoor radon was the second leading cause of lung cancer after cigarette smoking.

A recent study by two University of Iowa researchers, who were part of a large, multi-center study, provides compelling direct evidence of an association between prolonged residential radon exposure and lung cancer risk, according to a UI Health Care News release of March 21, 2005. The study, an analysis of data pooled from seven different

North American residential radon studies, demonstrates an 11 to 21 percent increased lung cancer risk at average residential radon concentrations of approximately 3.0 picocuries per liter of air (110 $Bq/m^3$), during an exposure period of five to 30 years. The lung cancer risk increased with increasing radon exposure. According to R. William Field, Ph.D., University of Iowa College of Public Health associate professor of occupational and environmental health and epidemiology, and a co-author of the study, the analysis which is based on the largest radon data set assembled in North America, agrees with a similar large-scale radon pooled analysis performed concurrently in Europe. The North American and European pooling provides unambiguous and direct evidence of an increased lung cancer risk even at residential radon exposure levels below the U.S. EPA's action level.

The Surgeon General Health Advisory on radon maintains that there is a national health problem associated with indoor radon gas; that radon exposure causes thousands of deaths each year; and elevated radon concentrations can be found in millions of homes (BEIR VI, 1999). All major health organizations, including the Centers for Disease Control and Prevention, The American Lung Association, and the American Medical Association, agree that radon-related deaths are preventable by decreasing the concentration and the exposure to the alpha particles released by radon and the radon decay products.

Recognizing indoor radon as a significant cause of lung cancer around the world, the World Health Organization (WHO), in collaboration with EPA and participating

countries, is launching and organizing an International Radon Project aimed at helping countries reduce the health risks associated with indoor radon, according to an EPA News Release of June 2005. The approach will focus on increasing public awareness about this invisible health threat and what can be done to reduce the risk. The World Health Organization estimates that radon could cause up to 15 percent of lung cancers globally.

Most European States and many non-European countries have recommended reference levels for dwellings and workplaces, and some have guidelines for measures against radon incorporated in their building codes and guidelines for construction techniques. EPA recommends that if radon is found above 148 $Bq/m^3$, you should fix your home. There is still some risk at level below 148 $Bq/m^3$, and EPA suggests that people may want to mitigate their homes to get them as close to ambient outside air as possible (outside air has approximately 14.8 $Bq/m^3$). The recommended action level by the IAEA in situations of chronic radon exposures within homes ranges from 200 to 600 $Bq/m^3$ of $^{222}Rn$ in air (EPA, 1986).

Other countries have adopted different action levels. Table 2.2 lists some of these international action levels (European Commission, 1998).

**Table 2.2: Comparison of International Radon Action Levels (European Commission, 1998)**

| | International Radon Action Levels | |
|---|---|---|
| | Existing Dwellings ($Bq/m^3$) | New Buildings $Bq/m^3$ |
| EU | 400 | 200 |
| ICRP | 200-600 | |
| WHO | 800 | 200 |
| Canada | 800 | 800 |
| Finland | 400 | 200 |
| Czech republic | 400 | 200 |
| Germany | 250 | 250 |
| Ireland | 200 | 200 |
| Norway | 400 | 200 |
| Sweden | 400 | 200 |
| Spain | 400 | 185 |
| Switzerland | 1000 | 400 |
| United Kingdom | 200 | 200 |

## 2.4 RADON STUDIES

Large-scale studies on indoor radon concentration have been carried out in Europe and in the United States, and the study has been steadily expanding throughout the world (Synnott *et al.*, 2006; El-Hussein *et al.*, 1998). These surveys range in type from small, localized short-term screening surveys to national surveys in which year long average indoor radon concentrations have been determined in randomly selected population weighed representative samples of national housing stock, which is the recommended methodology (UNSCEAR, 1993).

Radon concentrations in dwellings differ between countries because of differences in geology and climate, in construction materials and techniques, and in domestic customs. Published radon data for over 20 European countries indicate that the average radon concentration in homes varies widely, from less than 25 $Bq/m^3$ in the Netherlands, the UK and Cyprus to over 100 $Bq/m^3$ in Estonia, Finland, Sweden, Luxembourg, the Czech Republic, Hungary and Albania. Individual dwellings with radon gas concentrations above 10 000$Bq/m^3$ have also been found in Finland, Norway, Sweden, Belgium, Germany, Switzerland, the UK, the Czech Republic and Spain (UNSCEAR, 2000). A number of mean values for radon concentration in randomly selected dwellings in countries all over the world are listed in Appendix C.

The exposure of the populations in the Nordic countries (Denmark, Finland, Iceland, Norway and Sweden) to natural radiation sources is among the highest in the world and much effort has been devoted during the last 10 to 20 years to characterizing, assessing and, where feasible, to reducing these exposures. The exposure of workers to natural radiation sources has also been an important area of work in the same period. The Nordic Radiation Protection Authorities have recommended investigation level for radon in existing dwellings to be 200 $Bq/m^3$ and the action level of 400 $Bq/m^3$ while remedial measures in dwellings should be considered when the annual mean radon concentration in the living area exceeds 200 $Bq/m^3$. In the range between 200 and 400 $Bq/m^3$ simple, low cost measures are recommended. At levels exceeding 400 $Bq/m^3$, remedial measures should be undertaken with the aim of bringing the radon level below 200 $Bq/m^3$.

Remedial measures should be cost-effective and based on well-proven techniques (Akerblom *et al.*, 2000).

Radon concentration has been shown to vary seasonally. Mahmoud (2004) carried out a study to investigate seasonal variation of radon in Jordan. The average concentrations in dwellings in Jordanian cities ranged from about 20 to 386 $Bq/m^3$ with the highest readings exhibited during the winter season around the town of Al-Ruseifa. This was attributed to the meteorological conditions, since in winter, these dwellings were poorly ventilated to save energy but they had good ventilation in the summer time. Research carried out in the great pyramid "Cheops" of Egypt showed similar seasonal variation, where highest radon concentration values inside the pyramid were reported in winter, and lowest in summer (Hafez *et al.*, 2003).

Because radon levels may vary over short distances, it is recommended that testing be done in all buildings. A survey carried at Bryn Mawr College (Freidman, 2000) found radon levels in one building 20 times as high as those in an adjacent building, an observation that is consistent with research findings.

Models have been used to estimate indoor radon concentration in dwellings. Anastasiou *et al.* (2003) used a numerical model to calculate the airborne radon concentration in the interior of various Cypriot buildings and dwellings. The concentrations were found to be in the range of 6.2 to 102.8 $Bq/m^3$, with an overall arithmetic mean value of 19.3 $Bq/m^3$.

This value is by a factor of two below the world average (population weighted) value of 39 $Bq/m^3$.

Various authors (Ng *et al.*, 1995) have used calculations and measurements of concentrations of naturally occurring radionuclides in the building materials to estimate absorbed dose rates in dwellings. In these calculations, absorbed dose in air inside reference rooms of particular dimensions, wall thickness and materials' densities were determined per unit concentration of $^{40}K$, $^{226}Ra$ and $^{232}Th$ in the building materials. These values were then used to estimate organ dose rates or effective dose rates of dwellers of typical rooms made of materials with known concentrations of gamma emitting radionuclides.

## 2.5 BUILDING MATERIALS AS A SOURCE OF RADON

All building materials contain various amounts of natural radioactive nuclides. Materials derived from rock and soils contain mainly natural radionuclides of the $^{238}U$ and $^{232}Th$ series, and the radioactive isotope of $^{40}K$. In $^{238}U$ series, the decay chain segment starting from $^{226}Ra$ is radiologically the most important and, therefore, reference is often made to radium instead of uranium.

Elevated indoor radon levels may arise due to the use of building materials containing high levels of $^{226}Ra$. Examples of such materials are fly ash bricks, gypsum, alum shale, volcanic tuffs and pozzolana where radium and thorium content can reach some hundreds of Bq/kg (European commission, 2000; Battaglia *et al.*, 1990; UNSCEAR, 1982).

Another factor affecting indoor radon concentration is radon exhalation rate. Research carried out in Egypt indicated that building materials made from waste gypsum from fertilizer production facilities (phosphogypsum) showed increased rates of radon exhalation, compared to other building materials (Maged and Ashraf, 2005).

## 2.6 RADON SURVEYS IN KENYA

Little data is available in Kenya as far as natural radiation situation is concerned. Exposure to various components of the natural background radiation as reported by Mustapha (1999) indicated an average annual effective dose of 3.9 mSv/y in the country. In his report, a screening survey revealed radon concentration in indoor air to be in the range of 100 to 1160 $Bq/m^3$. Maina *et al.* (2004) investigated the radon concentrations in the coastal and rift valley regions of Kenya. Higher concentrations were found in the coastal region (43-704 $Bq/m^3$) while the Rift Valley region reported radon concentration of less than 100 $Bq/m^3$. The difference in radon concentrations in the two regions was attributed to geology and building designs.

In rural Kenya, modern buildings coexist with traditional huts. Those who are well off economically tend to use the traditional houses as kitchens, and retire later on in the modern houses. The design of the modern houses is basically the same, but different communities construct the traditional huts differently. Traditional way of life cannot be wished away, but people can be enlightened on the proper way of designing these houses for minimal radon concentration. In this study, radon concentrations in both modern and traditional houses are analyzed. Based on the results obtained, the local people can then be advised accordingly.

# CHAPTER 3

# THEORETICAL CONSIDERATIONS

## 3.1 RADON GENERATION AND TRANSPORT

Radon migration into dwellings depends on radon generation and transport in the underlying soil and porous building materials (Michel, 2003).

### 3.1.1 Radon Generation

Radon is one of the elements in the decay series of uranium that occurs as a trace element in almost all natural materials. The direct predecessor of radon in these series is radium, which is often incorporated in the solid matrix of soil and building materials. Before radon can enter the pore space of the material and become available for transport to the indoor environment, it has to escape the solid matrix of the particle.

Radon gas is transferred from the solid matrix into pore spaces (gas or liquid filled spaces between soil particles) primarily by alpha recoil. Alpha-particle recoil occurs after radium decays by emitting an alpha particle. After the particle is ejected, the resulting radon atom actually recoils in the opposite direction. Alpha-particle recoil results in breaking of chemical bonds in the solid, physically moving the atom to a different position and damaging the crystal structure.

The alpha decay of $^{226}$Ra is represented by the following equation:

$$^{226}Ra \rightarrow {}^{222}Rn + {}^{4}\alpha \qquad 3.1$$

The resulting particles ($^{222}Rn$ and $^{4}\alpha$) are charged and emitted with finite kinetic energy. During the decay, it is assumed that both total momentum and kinetic energy are conserved. Therefore, assuming that the nucleus was initially at rest, it follows that:

$$Q = \Delta Mc^2 = E_c^{Rn} + E_c^{\alpha} \qquad 3.2$$

$$M_\alpha V_\alpha = M_{Rn} V_{Rn} \qquad 3.3$$

Where $E_c$, M and V are the kinetic energy, the mass and the velocity of the daughter nuclide and the helium atom. From these equations, the kinetic energy of the daughter nuclide can be shown to be a small fraction of the total energy release Q:

$$E_c^{Rn} = Q\frac{M_\alpha}{M_\alpha + M_{Rn}} \qquad 3.4$$

The radon atom may recoil to a position from which it will not be released (embedded in the same particle or in another particle) or may recoil into the pore space and is available for transport. The recoil energy, due to the conservation of energy and momentum in the decay process, allows a radon atom to travel a certain distance in a porous material. The typical distance traveled is called the recoil-distance and depends on the material (phase) it travels through. The range of recoil distance for $^{222}Rn$ is 20-70 nm in common minerals, 100 nm in water and 63 μm in air (UNSCEAR, 2000). Although alpha recoil is believed to be the major process of radon release from solids, diffusion from very small

pores near the particle surfaces and along imperfections of the crystalline structure of the particle also occurs.

Not all radon produced in the particle enters in the pore space. The ratio between the amount of radon that becomes available for transport and the total amount of radon generated is called the emanation coefficient and is denoted by the letter $\eta$.

$$\eta = \frac{amount\ of\ radon\ aavailable\ for\ transport}{total\ amount\ of\ radon\ generated} \qquad 3.5$$

The radon emanation rates are known to strongly depend on the moisture content of the soil. A certain experiment has observed that the emanation coefficients increased with the increasing moisture content and then decreased before reaching saturated conditions. Grain size is another important factor controlling the soil's emanation coefficient. If $^{226}Ra$ is uniformly distributed throughout the soil grains, the emanation coefficient is inversely proportional to the grain radius. Several experiments have verified the theory mentioned above (Shweikani *et al.,* 1995; Martino *et al.,* 1998; Baixerax *et al.,* 2001). Once emanated in the pore space of the material, diffusion and advection are responsible for its transport and thus release.

### 3.1.2 Radon Transport in Porous Media

In order to enter the indoor air, radon must be transported, basically through the larger air-filled pores within the soil or building material, so that a fraction of them reaches the soil-air or building-air interface before decaying. There are two basic mechanisms of

radon transport within medium material: diffusion and advection (Graaf *et al.*, 1997; Richon *et al.*, 2003)

***Transport by Diffusion***

The primary transport mechanism of radon in a particular medium before decaying is done by the random molecular motion. Like any fluid substance there is a tendency to migrate in a direction opposite to that of the increasing concentration gradient within the material. This tendency is described by Fick's law, which relates the fluid flux density across the pore area to its concentration gradient. The coefficient relating these parameters is termed the effective diffusion coefficient, $D_e$, with a proper unit of $m^2$ /s and has an upper bound given by the diffusion coefficient in open air, $D_0$ often referred to as bulk diffusion coefficient. The bulk diffusion coefficient $D_0$ relates the interstitial concentration of radon to the flux density across a geometric area, $J_0$, whereas the effective diffusion coefficient relates the interstitial concentration to the flux density across the pore area, $J_e$ The most commonly used coefficient is $D_e$ and is related to the bulk diffusion coefficient in the following way:

$$D_o = \varepsilon D_e \qquad 3.6$$

Where $\varepsilon$ is the total soil porosity.

In this definition, the effective diffusion coefficient describes the actual transport rate for radon in the air-filled pore space rather than the bulk transport. The effective diffusion coefficient can, for example, be used to compare diffusion rates in materials with similar pore structure but different porosity. Typical values for the effective diffusion coefficient

for soil with relatively low moisture content, is of the order of $10^{-6}$ $m^2/s$. The diffusion coefficient for radon in air is about $1.2 \times 10^{-5}$ $m^2/s$.

According to the Fick's law, the diffusive flux density $\vec{j}_d$ ($Bq/m^2$ s), of radon or activity per unit of pore area is:

$$\vec{j}_d = -\vec{D}_e \nabla C \qquad 3.7$$

where C is the interstitial concentration of radon. The negative sign in front of the diffusion coefficient arises from the fact that the diffusion occurs in the opposite direction of the increasing concentration.

In the case where the transportation of radon is considered only in one direction, the differential equation for the diffusion is:

$$\frac{\partial C}{\partial t} = D_e \frac{\partial^2 C}{\partial x^2} - \lambda C + S \qquad 3.8$$

where $D_e$ is the effective radon diffusion coefficient, $C$ the radon concentration in pore space of the soil, x is the distance from the ground surface with the positive direction downwards; $\lambda$ is the radon decay constant and $S$ is the creation rate of radon per unit bulk volume, measured in $Bq/m^3$s and obtained from (Sun *et al.*, 2004):

$$S = \frac{A}{\varepsilon} \qquad 3.9$$

where $\varepsilon$ is the effective porosity of the soil/building material defined as the ratio of void volume to total volume and $A$ defined as equation 3.10 is the production of radon into the pore space:

$$A = \rho\lambda RE \qquad 3.10$$

where $\rho$ is the dry bulk density of the soil/building material, $R$ is the $^{226}Ra$ activity in the solid particles and $E$ is the radon emanation coefficient. The transport equation above is true when the only transport mechanism is diffusion and when the water content is negligible.

Let us assume that the soil is uniform. The radon concentration at the surface of the soil is $C_0$, whereas the radon concentration tends to a maximum constant value $C_{max}$, deeper underground. This implies that $C_0$ is less than $C_{max}$. The boundary conditions can then be stated as: $C\big|_{x=0} = C_0$ and $C\big|_{x\to\infty} = C_{max}$. It is also assumed that the system is in steady state, thus:

$$\frac{\partial C}{\partial t} = 0 \qquad 3.11$$

Applying equation 3.11, equation 3.8 can be written as:

$$D_e \frac{\partial^2 C}{\partial x^2} - \lambda C + S = 0 \qquad 3.12$$

Applying the boundary conditions, the solution for equation 3.12 is:

$$C = C_{\max} + (C_o - C_{\max}) \exp\left( - \sqrt{\frac{\lambda}{D_e}} x \right) \qquad 3.13$$

Assuming that the radon concentration is zero at the surface and that radon transport is by diffusion only, then:

$$C(x) = C_{\max} (1 - \ell^{-\frac{x}{l_d}}) \qquad 3.14$$

where

$$l_d = \sqrt{\frac{D_e}{\lambda}} \qquad 3.15$$

is the diffusion length. This corresponds to the distance at which the deep-soil $C_{max}$ is reduced by a factor of $1 - e^{-1}$. Taking as typical value for the effective diffusion coefficient, $D_e = 2 \times 10{-}6$ m$^2$/s (UNSCEAR, 2000), the value obtained for $l_d$ is ~97.6 cm for $^{222}$Rn.

***Transport by Advection***

When a fluid has a sufficiently low Reynolds number as is the case of $^{222}Rn$, transport through soil and building material, viscous and/or laminar fluxes may be induced due to a pressure gradient. This gradient could be created mainly by changes in meteorological conditions and the use of mechanical systems such as exhaust fans or blowers, heating and air-conditioned systems in dwellings. Advection takes place when there is pressure difference between the airs of pore space and ground surface. It is not limited to exchange of air between open spaces but can also be flow through porous materials such as soil and building materials. As a result, porous media act as sources of advective radon.

Pressure-driven convective radon flow can be characterized by Darcy's law, which relates the apparent velocity of fluid flow through a cross-sectional area to the pressure gradient, $\nabla P$ as follows:

$$\vec{q} = -\frac{\kappa}{\mu}\vec{\nabla}P \qquad 3.16$$

where $\vec{q}$ (m/s) is the Darcy's velocity vector, which is defined as the flow per unit geometrical area over an element of large volume relative to individual pores; $k$ ($m^2$) is the intrinsic gas-permeability; $P$ is the pressure field in units of Pa; and $\mu$ (Pa s) is the dynamic viscosity of the gas. In this equation the effect of gravity is neglected.

The advective flow density per unit of pore area is then:

$$\vec{J}_a = C\vec{q} = -\frac{C\kappa}{\mu}\vec{\nabla}P \qquad 3.17$$

where $\vec{J}_a$ is flux of radon in the air-phase as a result of advection (Bq/m$^2$s) and $C$ is radon concentration in the air-phase.

Advective transport is considered to be responsible for radon transport when high values of radon concentration are reported (UNSCEAR, 1993; UNSCEAR, 1988). The most important factor affecting advection is the soil permeability. Other meteorological parameters like temperature difference between soil and surface air, wind velocity and rainfall also affect the advection process.

## 3.2 PRINCIPLES OF GAMMA-RAY SPECTROMETRY

### 3.2.1 The Decay Law

Radioactivity is a spontaneous nuclear reaction that is unaffected by temperature, pressure or any other external variable. The equation of decay for a given number of atoms, $N$, of a given nuclide can be written as follows:

$$-\frac{dN}{dt} = \lambda N \qquad 3.18$$

where λ is the proportionality constant called decay constant, related to the half-life by $\lambda = ln2/t_{1/2}$ with $t_{1/2}$ being the half-life of the radionuclide. If the number of nuclei present at $t = 0$ is $N_0$ then upon integration, the decay equation becomes:

$$N = N_o e^{-\lambda t} \qquad 3.19$$

The natural unit of radioactivity is disintegration/time (dps or dpm). The SI unit is Becquerel (Bq) where: *1 Bq = 1dps*. Counting rates in a detection system are usually given in cps or cpm. It is very rare that every disintegration is counted. However proportionality exists for any detection system between absolute disintegration rate and the observed decay rate i.e., *dpm = εcpm*, where ε is the proportionality constant called detector counting efficiency. The counting efficiency depends on:

- Detector type
- Geometry of counting arrangement
- Type and energy of radioactive decay.

### 3.2.2 Secular Equilibrium

Let us begin by considering the case when a radionuclide, *a*, decays with a decay constant $\lambda_a$ forming a daughter, *b*, with a decay constant $\lambda_b$. We can write terms for production and depletion of *b*:

*Rate of change of b present at time* t = *Rate of production of b* - *Rate of decay of b*

i.e. $$\frac{dN_b}{dt} = \lambda_a N_a - \lambda_b N_b \qquad 3.20$$

where $N_a$ and $N_b$ are numbers of *a* and *b* present at time t.

The solution of equation 3.20 is:

$$N_b = \frac{\lambda_a}{\lambda_b - \lambda_a} N_a^0 \left( \ell^{-\lambda_a t} - \ell^{-\lambda_b t} \right) + N_b^0 \ell^{-\lambda_b t} \qquad 3.21$$

where $N_b^0$ is the number of species $N_b$ present at $t=0$. First term of (3.21) represents growth of daughter due to the decay of the parent while the second part represents the decay of any daughter initially present. Where the parent is far much more longer-lived than the daughter, it follows that $\lambda_a << \lambda_b$. In equations where there is no initial $N_b$ present, the second term can be dropped. With this in mind, equation (3.21) can be simplified to:

$$N_b = \frac{\lambda_a}{\lambda_b} N_a \left( 1 - \ell^{-\lambda_b t} \right) \qquad 3.22$$

Because the observation time is small, $N_a$ does not seem to change due its longer half-life, therefore $N_a^0 = N_a$. After about 7 half-lives of the daughters, $\ell^{-\lambda_b t}$ approaches zero and can be removed from equation (3.22), which becomes:

$$N_b = \frac{\lambda_a}{\lambda_b} N_a \qquad 3.23$$

This situation, when the activity of the higher atomic number nuclide, the "parent," is equal to the activity in the next step, the "daughter", is known as radioactive equilibrium (also referred to as secular equilibrium). Thus, secular equilibrium between a parent and a daughter implies the activity ratio is 1. This is illustrated in Figure 3.1 below.

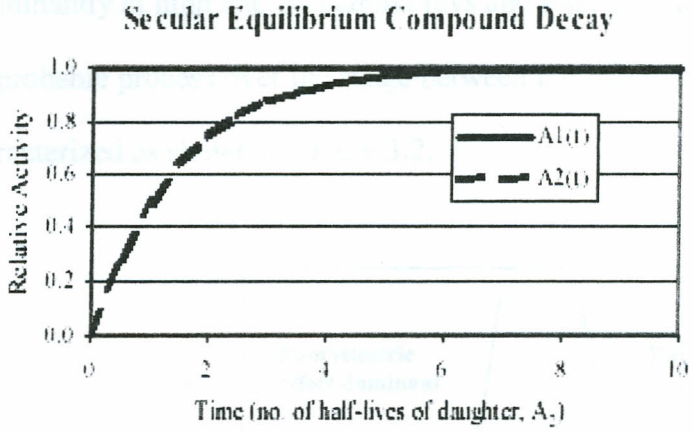


**Figure 3.1: Secular Equilibrium Compound Decay**

### 3.2.3 Gamma Rays

The gamma-ray energies emitted by various radionuclides are unique for each species, and are said to fingerprint the material. Determination of the quality and quantity of a gamma-ray spectrum can identify minute quantities of an element within an unknown sample. X-ray or gamma-ray photons are uncharged particles. They create no direct ionization or excitation of any material through which they pass. The detection of gamma rays is critically dependent on causing a gamma-ray photon to undergo an interaction that transfers all or part of the photon's energy to an electron in the absorbing material. Because the primary gamma-ray photons are "invisible" to the detector, it is the fast

electrons created in the gamma-ray interactions that provide information of the incident gamma rays.

The interaction mechanisms of gamma rays include photoelectric absorption (predominantly at low energy gamma rays and high $Z$ material), pair production (predominantly at high energy gamma rays and high $Z$ material), and Compton scattering (most probable process over the range between the two extremes). These interactions can be characterized as shown in Figure 3.2.

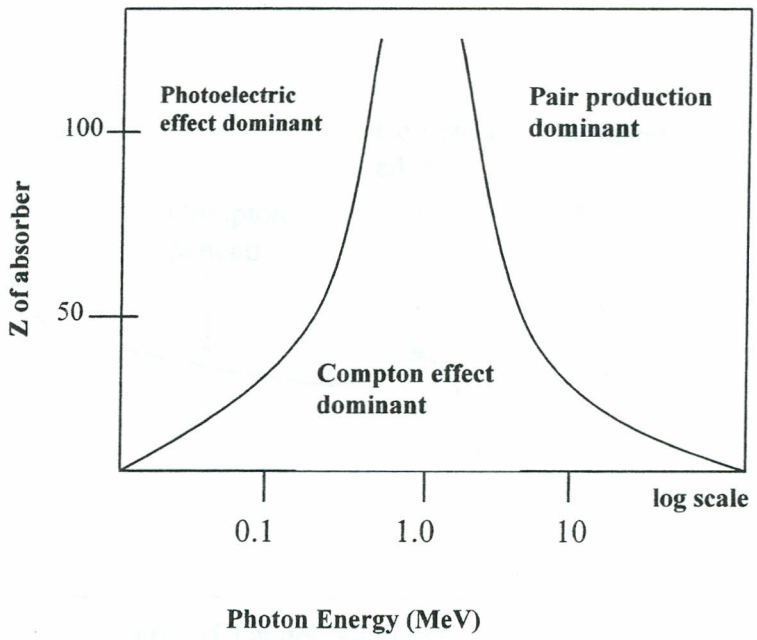


**Figure 3.2: Schematic Representation of the Three Major Types of Gamma Ray Interactions**

For a detector to serve as a gamma-ray spectrometer it must act as a conversion medium in which incident gamma rays have a reasonable probability of interacting to yield one or

more electrons and it must function as a convectional detector for these secondary electrons.

***Photoelectric Absorption***

When a gamma ray interacts with matter, it can cause an electron to be ejected from the absorbing atom. This is the process which usually occurs in the NaI(Tl) detector. The most obvious and simplest feature will normally be the photopeak due to the photoelectric effect, in which a gamma ray is completely absorbed by an electron. This is shown in Figure 3.3.

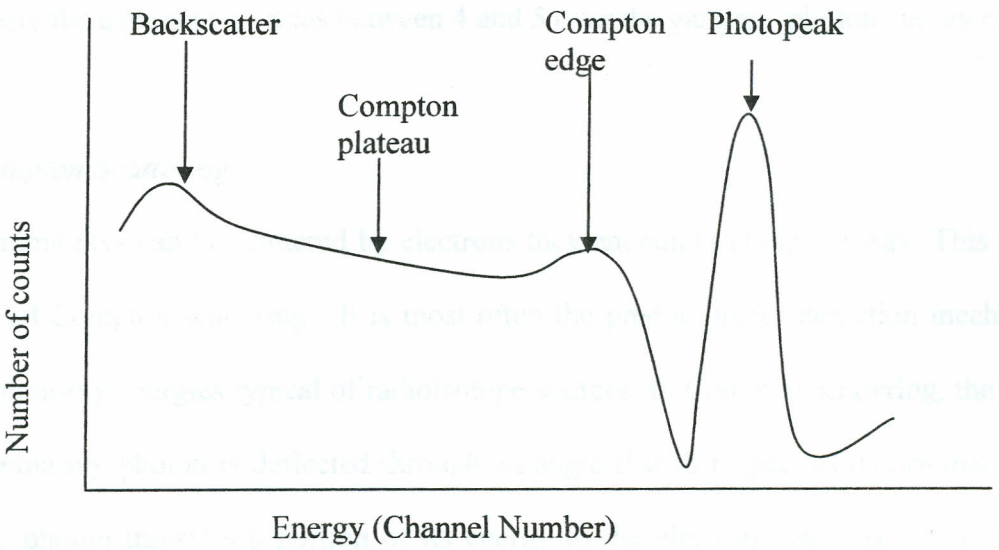


**Figure 3.3: Schematic Diagram of a Typical Gamma Ray Spectrum**

When all the electron energy is deposited inside the detector, the result is a sharp peak. The energy of the emitted photoelectron is:

$$E_e = h\nu - E_b \qquad 3.24$$

$E_b$ is the binding energy of the electron and $h\nu = E_\gamma$ is the energy of the incident photon. The probability of a photoelectric interaction (normally called the cross-section, $\tau$) depends on the atomic number $Z$ of the absorber and the energy $E_\gamma$ as shown below (Knoll, 1989):

$$\tau = \text{constant} \times \frac{Z^n}{E_\gamma^{3.5}} \qquad 3.25$$

where the exponent $n$ varies between 4 and 5 over the gamma –photon energy of interest.

***Compton Scattering***

Gamma rays can be scattered by electrons they encounter along the way. This process is called Compton scattering. It is most often the predominant interaction mechanism for gamma-ray energies typical of radioisotope sources. In Compton scattering, the incoming gamma-ray photon is deflected through an angle $\theta$ with respect to its original direction. The photon transfers a portion of its energy to the electron (assumed to be initially at rest), which is then known as recoil electron. Because all angles of scattering are possible, the energy transferred can vary from zero to a large fraction of the gamma-ray energy.

If the scattering is elastic, conservation of momentum and energy is used (bearing in mind that the velocities involved are relativistic) to derive an expression for the energy $E_\gamma'$ of the scattered gamma ray:

$$E_\gamma' = \frac{E_\gamma}{(E_\gamma / m_0 c^2)(1-\cos\theta)+1} \qquad 3.26$$

where $E_\gamma = h\nu$ is the energy of the incident gamma ray, $m_0c^2$ is the rest mass energy of the electron, and $\theta$ is the scattering angle.

The maximum transfer of energy to the electron and hence the minimum energy of the scattered gamma, occurs when $\theta = 180^0$. The energy of the electron is:

$$E_{ce} = \frac{E_\gamma}{(1+m_0c^2/2E_\gamma)} \qquad 3.27$$

This maximum $E_{ce}$ is called the Compton edge or Compton shoulder, and shows up as the high-energy end of the region of the spectrum due to Compton scattering in Figure 3.3.

The backscatter peak is created by Compton scattering in the material outside the detector, producing gamma rays that "ricochet" back into the detector and then undergo the photoelectric effect. The scattering angle still has a peak at $\theta = 180^0$ but now the energy observed is the original photon energy minus the maximum possible energy transfer to the electron. Then the energy of the scattered gamma ray is:

$$E_{bs} = E_\gamma - E_{ce} = \frac{E_\gamma}{(2E\gamma/m_0c^2)+1} \qquad 3.28$$

Compton interaction cross-section σ (Knoll,1989)

$$\sigma = \text{constant} \times \frac{Z}{E} \qquad 3.29$$

which increases linearly with atomic number, $Z$ of the absorber atom.

***Pair Production***

When gamma photon energy exceeds $2m_ec^2$ *(≥ 1.022 MeV),* the third type of photon interaction with matter is possible — pair production. In this process, photon is completely absorbed and its energy is turned into a creation of electron-positron pair, usually outside the detector.

The positron eventually slows and stops, then annihilates with a neighboring electron to produce two gammas with energy $E_{e+/e-}$ where:

$$E_{e+/e-} = m_ec^2 \qquad 3.30$$

These can subsequently be observed in the detector. Such photons could also Compton scatter, giving a second Compton edge and a second backscatter peak as described above, but with $E_\gamma = m_ec^2$.

The probability of pair production $k$ varies approximately as the square of the atomic number $Z$ of the absorber material (Knoll, 1989), i.e.

$$k \alpha Z^2 \qquad 3.31$$

### 2.2.4. Gamma-Ray Spectrometers

The range of γ-rays in a material is usually much longer than that for charged particles. Low-density detectors, such as gas tubes in Geiger-Müller counters, routinely used for detection of α or β radiation, have very low detection efficiency for gamma rays. Solids have sufficient density to absorb photons using even small size detectors. In gaseous detectors, ionization charge released in the absorption of nuclear radiation is easily collected with help of electric field applied to the detector. In conductors the ionization charge cannot be detected on top of the ordinary electric current flowing whenever electric field is applied. In insulators electrons cannot move at all. Semiconductors offer one possibility for construction of solid-state detector for nuclear radiation. Another type of solid-state detector is offered by scintillating materials. No external electrical field is required.

***NaI(Tl) Scintillation Mechanism***

Scintillators can be used not only to count nuclear radiation (like Geiger-Müller counters), but also to measure energy of the radiation. An approximately constant fraction of energy absorbed by the material is turned into scintillation photons. Since the energy needed to emit one scintillating photon is always the same, the total number of scintillation photons is proportional to the absorbed energy. The number of electrons

liberated by the scintillation photons on the photocathode of the photomultiplier is again proportional to the number of photons. Since every electron emitted by the photocathode goes through the same multiplication process in the system of dynodes, the total output from the photomultiplier is linearly proportional to the number of primary electrons, and thus to the energy absorbed by the scintillating material. Hence, the total charge produced on the output of the photomultiplier (PM) can be used to measure energy deposited by the nuclear radiation in the detector.

NaI(Tl) is an alkali halide inorganic scintillator. The scintillator mechanism depends on the energy states determined by the crystal lattice. This is as shown in Figure 3.4. Incident gamma-ray energy is absorbed and produces secondary electrons via photoelectric effect. The charged particles passing through the medium will form a large number of electron-hole pairs created by the elevation of electrons from the valence band to the conduction band.

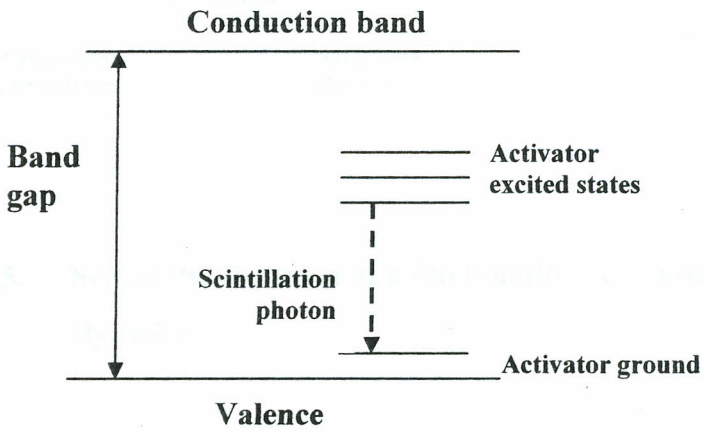


**Figure 3.4: Energy Band Structure of an Activate Crystalline Scintillator**

These electrons are then accelerated by the electric field created between the cathode and the first dynode. Kinetic energy of the accelerated electrons is used to liberate even more electrons when they strike the dynode. The first dynode is followed by another one and the multiplication process is repeated. Usually several stages of dynodes are used (Figure 3.5). The dynodes act as a series of accelerators through a high voltage to make these electrons very energetic. Eventually, electrons reach the anode. Thus, photomultiplier allows not only detection of the scintillation photons but also provides large signal amplification. The pulses of electrons are fed into a multichannel analyzer (MCA) which sorts them according to size, with bigger pulses going into higher numbered channels. Thus channel number is related to gamma-ray energy. The resulting spectrum will contain one or more photopeaks at the energies of the gamma rays emitted from the source.

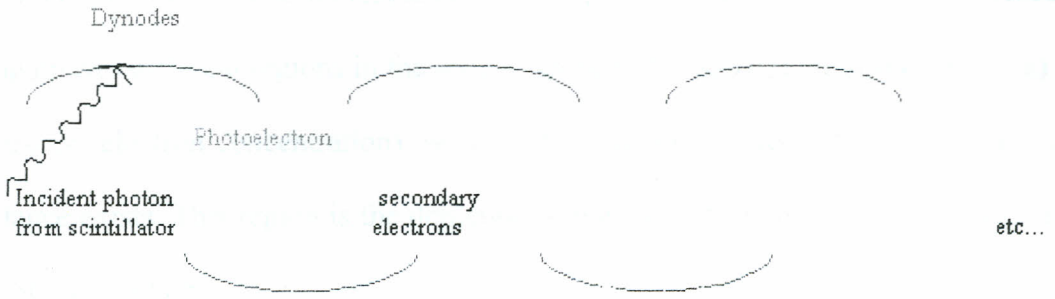


**Figure 3.5: Schematic Diagram of a Photomultiplier Tube with Succession of Dynodes**

The return of the electrons to the valence with the emission of a photon is an inefficient process. It can be enhanced by the presence of an activator. The activator, or an impurity

added to the inorganic material, creates energy bands in the band gaps through which the excited electron can de-excite back to the valence band. Because the energy is less than that of the band gap, this transition can now give rise to a visible photon and therefore serve as the basis of scintillation process.

NaI(Tl) has a number of properties that make it an excellent scintillator; it has a high scintillation efficiency (ability to create scintillations from the deposition of energy in the crystal), it has large photon production and it is transparent to its own scintillations. Unfortunately, NaI(Tl) is hygroscopic (readily absorbs water), so it must be sealed in a housing (usually aluminum) to keep it dry. They also have relatively crude energy resolution.

***Semiconductor Detector Mechanism***

The HPGe detector is a semiconductor diode type detector. The detector is formed by setting up two different regions in the semiconductor, "p" (excess hole concentration) and "n" (excess electron concentration), which have a region between them where a charge imbalance exists. This region is the depletion region, and it extends into both the p and n sides of the junction.

A p and n region adjacent to one another is called a junction. P connected to the positive and n connected to the negative is the forward bias. (The impedance across the junction is low and the current will flow across). If the number of charges on both sides is equal, the region is the same on both sides. Electron-hole pairs formed in the depletion region by

the electric field and their motion constitutes the basic electrical signal. Thus, the semiconductors provide a way to collect electrical charges created at either boundary of the semiconductor material.

By reverse biasing the p-n junction, very low current will cross the junction. The width of the depletion region increases and the noise properties of the semiconductor improve. When the reverse bias voltage is sufficient, the depletion region extends through an entire thickness of the wafer, resulting in a fully depleted detector. The depth of the depletion region is important to the type of radiation that can be detected. In the case of gamma spectroscopy, the depletion depth should be as large as possible. The thickness of the depletion region, $d$ is given by

$$d = \left( \frac{2\varepsilon V}{eN} \right)^{1/2} \qquad 3.32$$

where $\varepsilon$ is the dielectric constant of the medium, $V$ is the reverse bias voltage and $N$ is the net impurity concentration in the bulk semiconductor material. Gamma radiation requires greater depletion depths. Greater depletion depths are obtained by lowering $N$ through further reductions in the net impurity concentration.

Germanium is of high purity. However it is further processed to higher purity by the process of zone refining. The impurity levels are progressively reduced by locally heating the material and slowly passing a melted zone from one end of the sample to the other. Since impurities tend to be more soluble in the molten germanium than in the solid,

impurities are preferentially transferred to the molten zone and are swept away from the sample. Because of the small band gap (~0.7 eV), room temperature operation of a germanium detectors of any type is impossible because of the large thermally induced leakage current that would result. The HPGe must be cooled through the use of liquid nitrogen to reduce leakage current. The detector must be placed in a vacuum tight cryostat to inhibit thermal conductivity between the crystal and the surrounding air.

The detector uses coaxial geometry in which the outer surface serves as one electrode and a central conducting cylindrical core as the other electrode. A high voltage is applied between them. Gamma rays deposit their energy in the germanium and produce free electrons and holes (vacancies where the electrons were located in the crystalline germanium). The electrons and holes behave as negative and positive charges and are collected at the electrodes by the applied voltage. The amount of charge collected is correlated with the amount of energy deposited in the detector and therefore with the energy of the gamma ray that caused it. The detectors are used with multichannel analyzers to sort the pulses according to pulse height.

It requires a lot less energy to create an electron-hole pair in semiconductor detectors than it does in scintillation detectors such as NaI(Tl) detector and, mostly for this reason, the germanium detector has a much better resolution than NaI(Tl) detector. This means that if multiple gamma ray energies are being analyzed simultaneously, the germanium detector will do a better job at separating them cleanly.

Because the likelihood of gamma-ray interaction depends strongly on the atomic number of the material they are interacting with, the detection efficiency of germanium is considerably lower than that of NaI(Tl) detector because germanium has a much lower effective atomic number. One practical disadvantage of the germanium detector is that it must be operated at liquid nitrogen temperature to keep the thermal noise at an acceptably low level.

# CHAPTER 4

# MATERIALS AND METHODS

Indoor radon concentrations were measured using activated charcoal canisters and NaI(Tl) gamma ray detector while the presence of naturally occurring radionuclides in selected building materials like building stones, plaster, concrete, and mud were measured using HPGe detector. The sampling sites were selected such that it was possible to assess the influence of meteorological variables and construction detail to indoor radon concentrations.

## 4.1 EQUIPMENT AND MEASUREMENTS PROCEDURES

### 4.1.1 NaI(Tl) Gamma Ray Spectrometer for Measurement of $^{222}Rn$

The gamma-ray spectrometer consists of a shielded 76 mm x 76 mm NaI(Tl) detector. The detecting system also includes an oxford PCA-P Multichannel Analyser (MCA) card and its software. The PCA-P contains a high voltage power supply, a charge sensitive pre-amplifier, a shaping amplifier, 80 MHz Wilkinson analogue-to-digital converter (ADC) with multi channel analyser. The PCA-P card using a PC performs the data acquisition and analysis. Figure 4.1 is a block diagram showing the components of the gamma-ray spectrometer.

The spectrometer was calibrated using standard radioactive sources. The gamma lines used for calibration were 661.66 keV (from $^{137}Cs$), and 1173.24 keV and 1332.5 keV (from $^{60}Co$). It's counting efficiency ($\varepsilon$) was determined by counting a dry radon standard canister. The standard canister contains charcoal material, of similar composition and

quantity as the EPA canister used in this research, but spiked with known concentration of $^{226}Ra$ solution (Mustapha *et al.*, 1999).

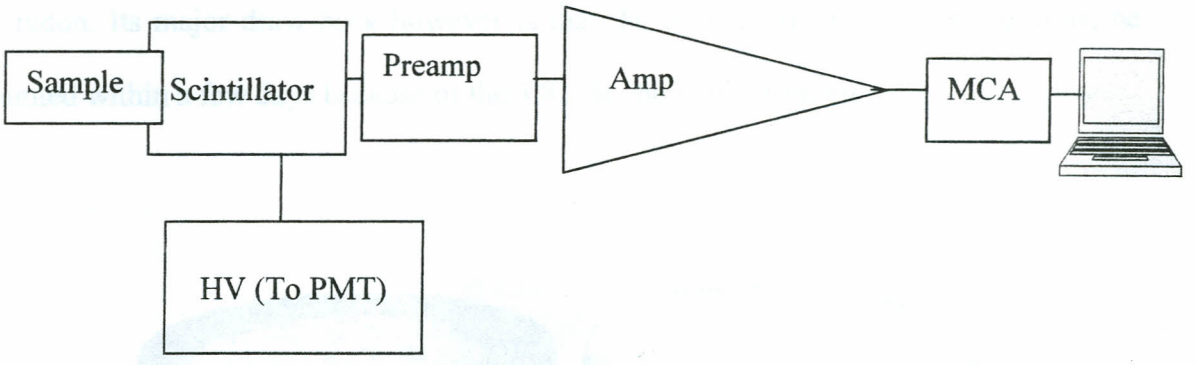


**Figure 4.1: A Schematic Diagram of NaI(Tl) Gamma Ray Spectrometer**

The counting efficiency was obtained from the equation below:

$$\varepsilon = \frac{N}{D} \qquad 4.1$$

Where $N$ = net counts per second and $D$ = disintegration per second of the standard canister.

The standard EPA charcoal canisters were used for radon sampling. The canister (Figure 4.2) consists of 8 ounce metal can with lid (4 inch in diameter and 11/8 inch deep), 70 ± 1g of 6 x 16 mesh activated charcoal, metal screen, removable internally expanding retaining ring, pad material attached to the inner surface of the lid, and a 13 inch strip pliant vinyl tape. The high affinity of activated charcoal for water vapour has been adapted in the measurement of radon in air (Mustapha *et al.*, 1999).

The charcoal canisters were found to be the most appropriate because of the simplicity as well as the economy of the technique. The sensitivity of the charcoal canister is the best of all other radon methods and devices in terms of net counts per minute per 148 $Bq/m^3$ of radon. Its major draw back however is that the analysis time is crucial i.e. must be counted within a few days because of the 3.82 day half-life of radon.

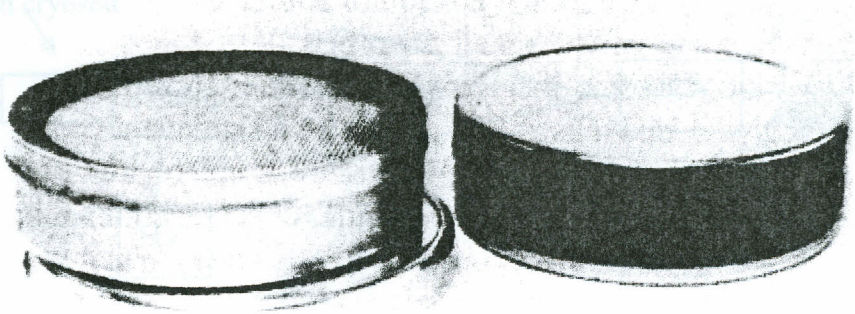

**Figure 4.2: Charcoal Canisters**

### 4.1.2 High Purity Germanium (HPGe) Detector for Measurement Of $^{226}Ra$, $^{232}Th$ And $^{40}K$

A high purity germanium (HPGe) detector, with an energy resolution of 1.83-2.2 keV FWHM at 1332 keV of $^{60}Co$ line and detection efficiency of about 20-30% relative to a 76mm x 76mm NaI(Tl) scintillator was used. The detector is mounted on cryostat that is dipped in to a 30L dewar filled with liquid nitrogen. It's surrounded with a lead shield that supplies an efficient suppression of gamma radiation present at the laboratory site.

Experimental arrangement for the spectra collection includes a high voltage detector bias supply and signal processing electronics. The spectral data analyses were performed with Oxford PCA3 multi–channel analyzer and the IAEA-GANAAS software. The electronic set-up for HPGe detector is as shown on a block diagram (Figure 4.3).

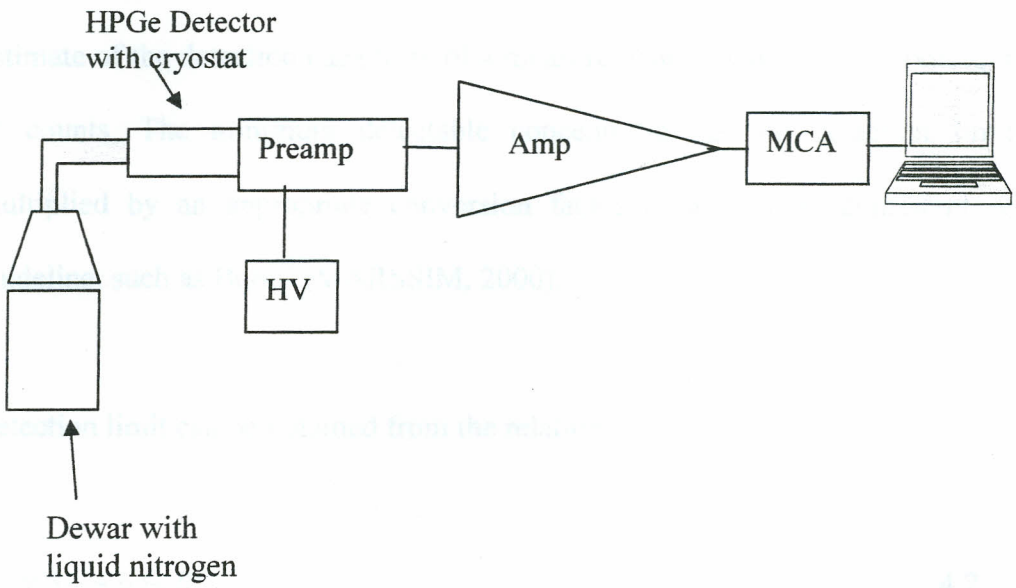


**Figure 4.3: A Schematic Diagram of HPGe Gamma-ray Spectrometer**

The spectrometer was calibrated using SRM-1 reference materials obtained from IAEA. The gamma lines used for calibration were 59.54 keV (from $^{241}$Am), 661.66 keV (from $^{137}$Cs), and 1173.24 keV and 1332.5 keV (from $^{60}$Co). To maintain reproducible geometry, equal volumes of samples and standards were used. Reproducible positioning of samples was ensured with the platform that holds sample container coaxial with the detector during counting.

***Detection Limits***

Radioactive decay is a random process that lends itself to statistical analysis. Because of this randomness of decay, limits or decision points must be calculated to determine whether or not activity exists in the sample or whether the counts fall within acceptable parameters for random background variations. Such analyses include the detection limit and the minimum detectable concentration *(MDC)*. The detection limit is defined as an estimate of the detection capability of a measurement system, and is reported in the units of counts. The minimum detectable concentration is the detection limit (counts) multiplied by an appropriate conversion factor to give units consistent with a site guideline, such as $Bq/m^3$ (MARSSIM, 2000).

Detection limit can be obtained from the relation:

$$L_D = 3 + 4.65\sqrt{B} \qquad 4.2$$

where $B$ is background counts. In Curie's derivation the constant factor of 3 in the $L_D$ formula was stated as 2.71, but since then it has been shown and generally accepted that a constant factor of 3 is appropriate (MARSSIM, 2000). The detection limits $L_D$ for the HPGe detector were evaluated from equation 4.2.

When the sample count times and background count times are different, the *MDC* formulation is used. The *MDC* can be obtained from equation 4.2 multiplied by a factor; C to convert from counts to concentration as shown in equation 4.3:

$$MDC = C \times (3 + 4.65\sqrt{B}) \qquad 4.3$$

The *MDC* of the NaI(Tl) detector system used in this study is shown in equation 4.4 (Mustapha *et al.*, 1999):

$$MDC = \frac{1000}{t_e.\varepsilon.CF.DF}\left(\frac{3}{T} + 4.65\sqrt{\frac{B}{T}}\right) \qquad 4.4$$

where, $t_e$ is exposure time in minutes, $\varepsilon$ is the counting efficiency, $CF$ is the calibration factor, $DF$ is the decay factor, and $T$ is the background count time.

## 4.2 SAMPLING AND SAMPLE PREPARATION

### 4.2.1 Indoor Air

Activated charcoal canisters, which are short-term integrating devices, were employed in the detection of $^{222}Rn$ in selected dwellings. These dwellings included model traditional huts and classes located in Kenyatta University, and basement rooms located at Chiromo campus of the University of Nairobi. The canisters were first activated by heating them in an oven at $100^0C$ for a period of 12 hours. This was to ensure that all moisture and radon initially present in the charcoal granules was driven off. This being the case, the mass of the canisters usually remains constant after activation.

The canisters were weighed before exposure, and they were exposed to radon in air at the sampling site for a period of 48 hours. At the exposure sites the canisters are placed at about 1 m above the ground and from the walls of the buildings. After exposure, the canister were resealed and reweighed. They were then left for about 3 hours to allow for equilibrium between radon and its daughters. Radon concentration was then determined by counting the gamma-ray emissions of $^{214}$Bi (609 KeV) using a NaI(Tl) gamma-ray spectrometer. The original radon concentration was determined based on exposure time and the calibration factor (*CF*).

The calibration factor is a measure of the response of the charcoal canisters; it depends on the length of time the canister is exposed and on the amount of water gained during the exposure. Basically, calibration procedure entails exposing samples of charcoal to a constant concentration of radon over different periods of time under controlled humidity in the laboratory exposure chambers. The initial calibration factor ($CF_i$) in L/min is then calculated from:

$$CF_i = \frac{N}{t_e.\varepsilon.Rn.DF} \qquad 4.5$$

Where $N$ is ther net counts per minute.

The decay factor is used to correct for the radioactive decay during the sampling period and is given by:

$$DF = \exp\left(\frac{-0.693t_d}{T_{1/2}\ for\ radon}\right) = \exp\left(-0.0075t_d\right) \qquad 4.6$$

Where $t_d$ = time from midpoint of exposure to the start of counting (min) or decay time and $T_{½}$ = half-life of $^{222}Rn$ in minutes = 5501 min.

The effect of humidity on the *CF* can be established by making runs at different humidity in controlled radon chambers. But since such facilities are not available the calibration data developed with similar canisters presented by the Eastern Environmental Radiation Facility (EERF) in the standard operating procedure manual was used in this study. This data relates weight of water absorbed to a calibration factor and was used to obtain the initial calibration factor $CF_i$. The final calibration factor, *CF*, was obtained by adjusting $CF_i$ for the actual exposure time;

$$CF = CF_i \frac{AF(t = t_e)}{AF(t = 48\,hours)} \qquad 4.7$$

Where $AF(t = t_e)$ and $AF(t = 48\ hours)$ are the adjustment factors for the actual exposure time $(t_e)$ and for 48 hours (optimum time) respectively.

The activity concentration, *C* (Bq $m^{-3}$), of radon in the air in which the test was carried out was be obtained from:

$$C = \frac{1000.N}{t_e.\varepsilon.DF(CF)} \qquad 4.8$$

### 4.2.2 Building Material

Samples of the different building materials were carefully collected. Samples from different places of the same material were then mixed together. A total of 7 samples were collected which represented the typical building materials used in Kenya. The soil samples were collected from the walls of the model traditional huts. Scoops of debris of dried up mud from walls of the huts were also collected. They were then thoroughly mixed together to form one homogeneous sample of about 5kg. Pieces of building stones and concrete blocks, plaster, concrete and sand were collected at construction sites and around existing buildings in Kenyatta University and the neighboring estates.

Each sample was crushed, sieved through a fine mesh and then left to dry for about one week. A part of each sample was packed in standard 450 ml marinelli beaker. These were then sealed, dry weighed and stored for 3 weeks before counting in order to allow in-growth of $^{226}$Ra and $^{232}$Th decay products and achievement of equilibrium for $^{226}$Ra and $^{232}$Th with their respective progeny. Each sample was then put in a shielded HPGe detector and measured for a period of 12 hours. Prior to samples measurement, the environmental gamma background at the laboratory site had been determined with an empty marinelli beaker under identical measurement conditions. It was later subtracted from the measured gamma-ray spectra of each sample. Based on the measured gamma ray photopeaks emitted by the radionuclides in the $^{232}$Th and $^{226}$Ra decay series and in the $^{40}$K present in the samples and the standard reference material, their radiological concentrations (in Bq/kg) were determined using the following relation:

$$\frac{A_s M_s}{I_s} = \frac{A_R M_R}{I_R} \qquad 4.9$$

where $A_s$ is the current activity of the specific radionuclide in the sample, $M_s$ is the mass of the sample, $I_s$ is the intensity of the sample, $A_R$ is the current activity of the specific radionuclide in the reference sample, $M_R$ is the mass of the reference sample, and $I_R$ is the intensity of the reference sample. Calculations relied on establishment of secular equilibrium in the samples, due to the much smaller lifetime of the daughter nuclides in the decay series of $^{232}$Th and $^{226}$Ra. More specifically, the $^{232}$Th concentration was determined from the average concentration of $^{228}$Ac (911 keV) in the samples, $^{226}$Ra was determined from the average concentration of $^{214}$Bi (1764 keV), and $^{40}$K was determined from 1461 keV. Figure 4.4 shows a typical gamma-ray spectrum from a mud sample.

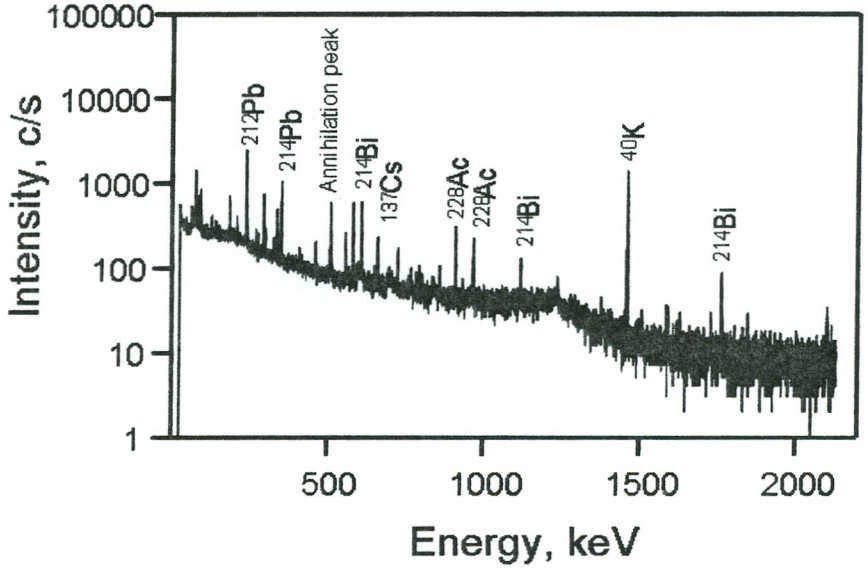


**Figure 4.4: Gamma-ray spectrum from a Mud Sample**

Also, approximately equal volumes of samples were selected for exhalation measurements. Each sample was carefully wrapped with tissue in order to reduce exhalation other $^{220}Rn$ and $^{219}Rn$. The samples were put in turns in a container, which was then tightly sealed and placed on the NaI(Tl) detector for the in-growth of radon concentration monitoring for several days. The ingrowths in counts for the different building material samples were then compared.

# CHAPTER 5

# RESULTS AND DISCUSSION

## 5.1 QUALITY CONTROL AND ASSURANCE

To ensure reproducibility of the measurements, various analytical control and assurance procedures were applied to the sample preparation and analytical procedures. The detection limits of both HPGe and NaI(Tl) detectors were determined. This allows for the determination of whether or not the calculated activity exists in the sample or whether the counts fall within acceptable parameters for random background variations.

The detection limit of the NaI(Tl) detector for the measurement of $^{222}$Rn was found to be 30 Bq/m$^3$. The detection limits of HPGe detector for the measurement of $^{226}$Ra, $^{232}$Th and $^{40}$K is summarized in Table 5.1.

**Table 5.1: Mean Detection Limits of Gamma-ray Spectrometer**

| *Radionuclide* | *Detection Limit (Bq/kg)* |
|---|---|
| $^{226}$Ra | 9.7 ± 2.1 |
| $^{232}$Th | 7.2 ± 1.8 |
| $^{40}$K | 7.4 ± 0.4 |

## 5.2 CONCENTRATIONS OF $^{222}$Rn IN SELECTED DWELLINGS

Results of $^{222}$Rn measurements in selected dwellings in Kenya are shown in Table 5.2 together with the arithmetic mean (A. M.), standard deviation (S. D.), the minimum

(Min) and maximum (Max) $^{222}$Rn concentrations. The histogram of $^{222}$Rn concentrations is depicted in Figure 5.1. The frequency of radon concentration was normally distributed, with a skew towards higher concentrations.

At the onset of sampling, the environmental conditions were very variable, with dry season giving way to the rainy season and eventually to the cold season. This happened within the span of two months hence the change in radon concentration. However, during the last month of sampling, the weather conditions less variable.

**Table 5.2: Activity Concentrations of $^{222}$Rn in Selected Dwellings in Kenya**

| | $^{222}$Rn concentration (Bq/m$^3$) | | | |
|---|---|---|---|---|
| | A. M. (Bq/m$^3$) | S. D. (Bq/m$^3$) | Min (Bq/m$^3$) | Max (Bq/m$^3$) |
| **Maasai hut** | 170 ± 13.8 | 61.8 | 80.2 | 286.5 |
| **Luo hut** | 183 ± 11.2 | 50.2 | 81.6 | 277.3 |
| **Kikuyu hut** | 150 ± 15.0 | 67.0 | 30.2 | 315.4 |
| **Luyha hut** | 178 ± 13.9 | 62.3 | 89.4 | 292.2 |
| **Classroom** | 193 ± 19.3 | 61.1 | 115.76 | 257.2 |
| **Basement room** | 202 ± 20.4 | 33.0 | 162.3 | 233.1 |

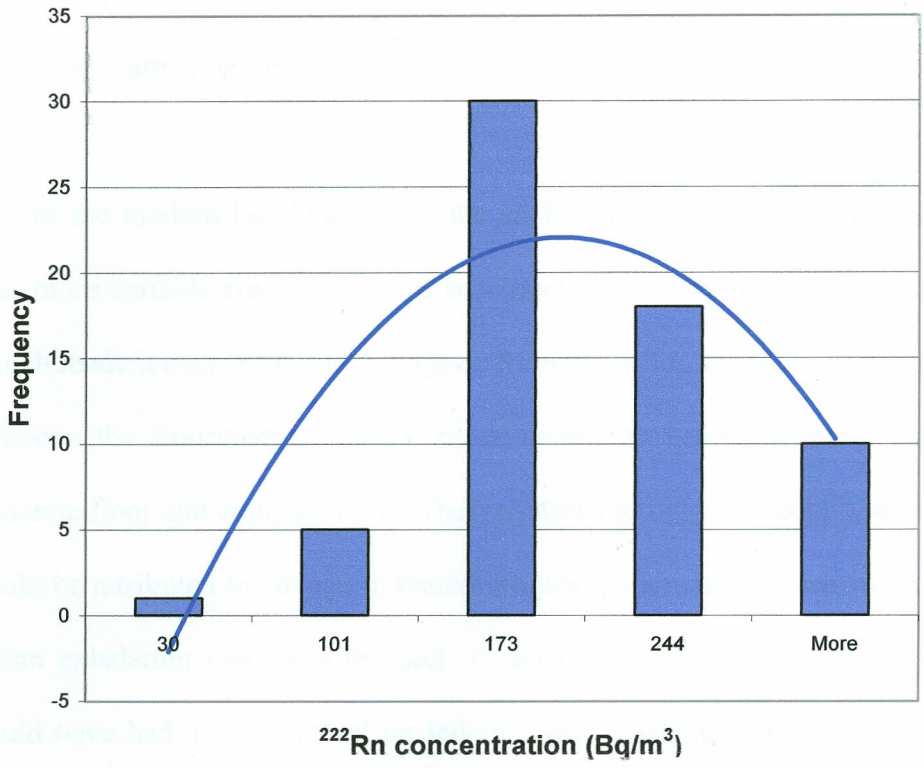


**Figure 5.1: Frequency distribution of $^{222}Rn$ concentration in selected Kenyan dwellings**

Radon concentration in the dwellings ranged from 30.2 Bq/m$^3$ to 315.4 Bq/m$^3$, with an overall arithmetic mean 172 ± 14 Bq/m$^3$. Out of all the buildings measured in this study, the basement room registered the highest mean radon concentration of 202.4 Bq/m$^3$ while the Kikuyu hut recorded the lowest concentration of 150.18 Bq/m$^3$.

The high radon concentrations in the basement room could be attributed to poor ventilation as the room remained shut through out the measurement period. The low variation could be attributed to the fact there was little influence of outdoor weather

conditions to indoor air in the basement room, as the temperature of the basement room remained more or less constant.

Out of the modern buildings under the study, the radon concentration in the classroom was more variable compared to the basement room. The classroom had a wooden floor, which made it easy for radon to migrate from the soil to the indoor air, through the cracks between the floorboards. On the other hand, the basement was more airtight, with concrete floor and concrete roof. The variations in radon concentration in the classroom could be attributed to change in meteorological parameters, which would possibly affect radon exhalation rate from the soil. A decrease/increase in soil radon exhalation rate could have had a direct effect on indoor radon concentration due to the easy routes of entry.

The variation in radon concentration was highest in the Kikuyu hut, with concentration ranging from 30.2 $Bq/m^3$ to 315.4 $Bq/m^3$ and lowest in the basement room (162.3-233.2 $Bq/m^3$). The two dwellings were therefore investigated further to find out if there was a reason for the varied radon concentration. It was discovered that part of the Kikuyu hut wall (which was built of mud) would soak up with rainwater following heavy downpour.

Though the effect of moisture on Kikuyu wall was not quantitatively determined the effect of moisture of the Kikuyu wall on the radon concentration, strong evidence pointed to the soaking of the wall as the possible cause of variation in radon concentrations. The level of radium in mud was found to be very high (Table5.3) and so was the exhalation

rate. Earlier discussions indicate that indoor radon concentration is affected by the radon exhalation rate from the building materials. The radon exhalation rate is affected by moisture content and radium concentrations, among other factors. Moisture increases the emanation rate of radon. Depending on the level of moisture, there can either be an increase or a decrease in radon exhalation rate, and this could have influenced the sudden surge in radon concentration in the Kikuyu hut.The argument was further supported by the fact that the variation of radon concentration in the Kikuyu hut was very similar to that in the Luo hut (Figure 5.2). This was not surprising because the two huts are similarly designed, with size and indoor partitioning (and to this effect ventilation) being the only difference. Though the radon concentration in the Kikuyu hut was lower than that of the Luo, there were occasional rises in the concentration, which could only be attributed to the effect of moisture on the walls of the Kikuyu hut.

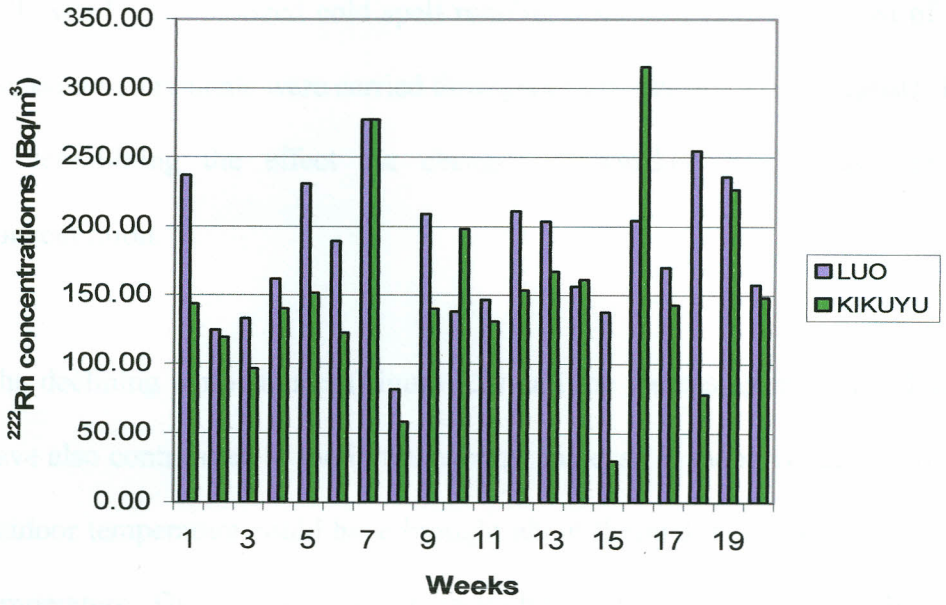


**Figure 5.2: Activity Concentrations of $^{222}Rn$ in the Kikuyu and Luo Model Traditional Huts**

Some statistical tests (ANOVA, F-test) on radon concentrations in the dwellings studied were carried out. The tests showed that the variation in radon concentrations between the dwellings was statistically insignificant compared to variation within the dwellings. The variation in radon concentrations between the Luo and the Kikuyu huts was however found to be statistically significant. Basically, the Kikuyu and the Luo huts have the same design as can be seen in appendix B1 and B2. The Luo hut is bigger in size. It is however partitioned in to small, poorly ventilated rooms and it is in one of these small rooms that sampling was done. The Kikuyu hut on the other hand, though smaller in size is more aerated as partitioned is done using sticks. This could explain the similar variation in indoor radon concentration in the two huts.

When measurements started (April, 2005), the rainy season was just setting in. This was followed by a prolonged cold spell running from mid-June to August of the same year. Radon measurements were carried throughout this period (April-August). This was aimed at determining the effect the changes in weather would have on indoor radon concentration.

The declining temperatures (Figure 5.3) and the increasing moisture (Figure 5.4) could have also contributed to the initial average increase in radon concentrations Reduction in outdoor temperature could have brought about thermal gradient due to the higher indoor temperature. This can bring about stack effect which can draw radon from the soil in the indoor air. However, level of radon soil during the cold season is usually low. This is

because the soil is wet, humid and of lower porosity that may decrease the diffusion of radon gas. The exhalation rate of radon is usually maximum in moist warm soils than in cold dry/soaked soil (Shweikani *et al.*, 1995). This could explain why eventually, the variation in mean radon concentration reduces, despite the persistent drop in temperatures.

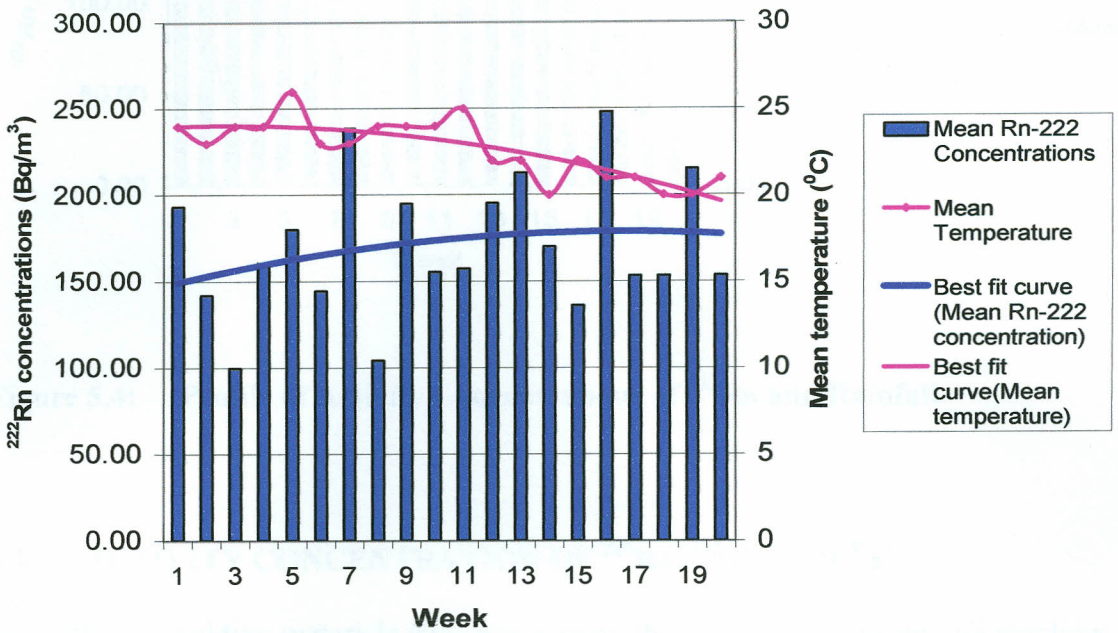


**Figure 5.3: Profile of Activity Concentrations of $^{222}Rn$ and Mean Temperature**

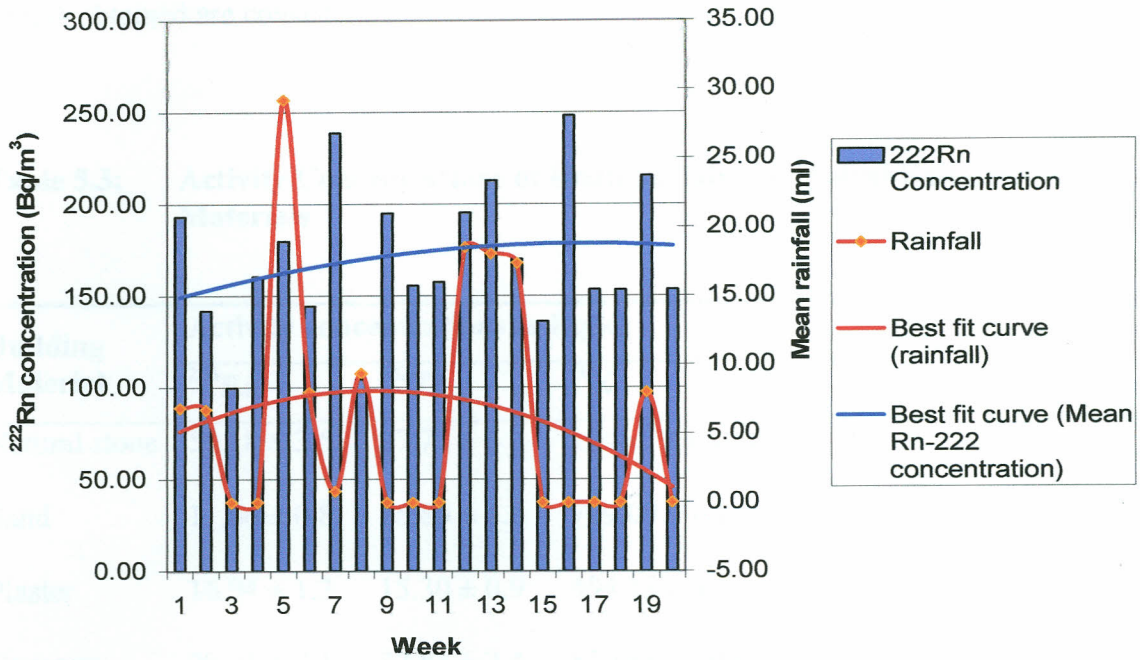


**Figure 5.4: Profile of Activity Concentrations of $^{222}$Rn and Rainfall**

## 5.3 ACTIVITY CONCENTRATION OF $^{226}$Ra, $^{232}$Th AND $^{40}$K

The different building materials analyzed contain the naturally occurring radionuclides in different proportion. The activity concentration in typical building materials were determined by comparison method using IAEA-375 reference material.

The activity concentrations of $^{226}$Ra, $^{232}$Th and $^{40}$K are shown in Table 5.3. Radioisotope activities in Bq/kg lie in the range of 11–101 for $^{226}$Ra; 15–148 for $^{232}$Th; and 295–1246 for $^{40}$K. Mud, which is used to make the walls of the huts, was found to have very high $^{226}$Ra and $^{232}$Th but low in $^{40}$K. Cement was also found to be high $^{226}$Ra in but low on $^{40}$K. Natural stone was found to be high in $^{40}$K. So were sand, concrete premix and

concrete blocks. Concrete is mainly made up of sand and pieces of stones; therefore the results obtained are consistent.

**Table 5.3: Activity Concentrations of Radionuclides in Typical Building Materials**

| Building Material | Activity concentrations in Bq/kg | | |
|---|---|---|---|
| | $^{226}Ra$ | $^{232}Th$ | $^{40}K$ |
| Natural stone | 50.18 ± 3.5 | 97.73 ± 6 | 1246.79 ± 10.0 |
| Sand | 11.66 ± 0.8 | 26.80 ± 1.6 | 799.09 ± 6.8 |
| Plaster | 16.94 ± 1.2 | 15.30 ± 0.9 | 494.12 ± 4.5 |
| Concrete | 29.05 ± 2.1 | 37.83 ± 2.4 | 810.64 ± 10.6 |
| Mud | 101.93 ± 7.1 | 148.34 ± 8.9 | 295.60 ± 4.5 |
| Bricks | 23.01 ±1.6 | 53.41 ± 3.2 | 806.04 ± 8.6 |
| Cement | 72.13 ± 5 | 32.32 ± 1.9 | 254.46 ± 1.8 |

Other than cement and plaster premix, all the other building materials had higher $^{232}Th$ concentrations than $^{226}Ra$ concentrations. This is consistent with other reports identifying various types of rock (which eventually form soil, sand and building stones) in Kenya with minerals and accessories like sphene, zircon, monazite, nepheline and microcline, which are known to be richer in radium and thorium (Mustapha *et al.*, 1999).

The high radium content in mud could be attributed to the clay soils it was obtained from. Clay soils are known to contain high levels of radium and low levels of potassium. The activity concentrations of the radionuclides present in natural stone, concrete mud and

bricks are within the concentration bracket obtained by Mustapha *et al,* 1999. Generally, the most abundant radionuclide in the building materials is potassium followed by thorium and finally radium as can be seen in Table 5.4.

**Table 5.4: Average Activity Concentrations of Naturally Occurring Radionuclides in selected Building Materials**

| Radionuclide | Average activity concentration (Bq/kg) |
|---|---|
| $^{226}Ra$ | 43.6 ± 3 |
| $^{232}Th$ | 58.8 ± 3.6 |
| $^{40}K$ | 672.4 ± 6.7 |

## 5.4 EXHALATION RATES

The contribution of building material to indoor radon is dependent on the radium concentration, the structural characteristic of the building material like porosity, moisture content and finishing, and on the prevailing atmospheric conditions like temperature and pressure. We set out to find out which among some typical building materials had the highest exhalation rate. This was done by sealing samples of almost equal volumes in a container and then recording the rate at which the number of radon atoms are changing inside the container over a period of several days. The results are shown in Figure 5.5.

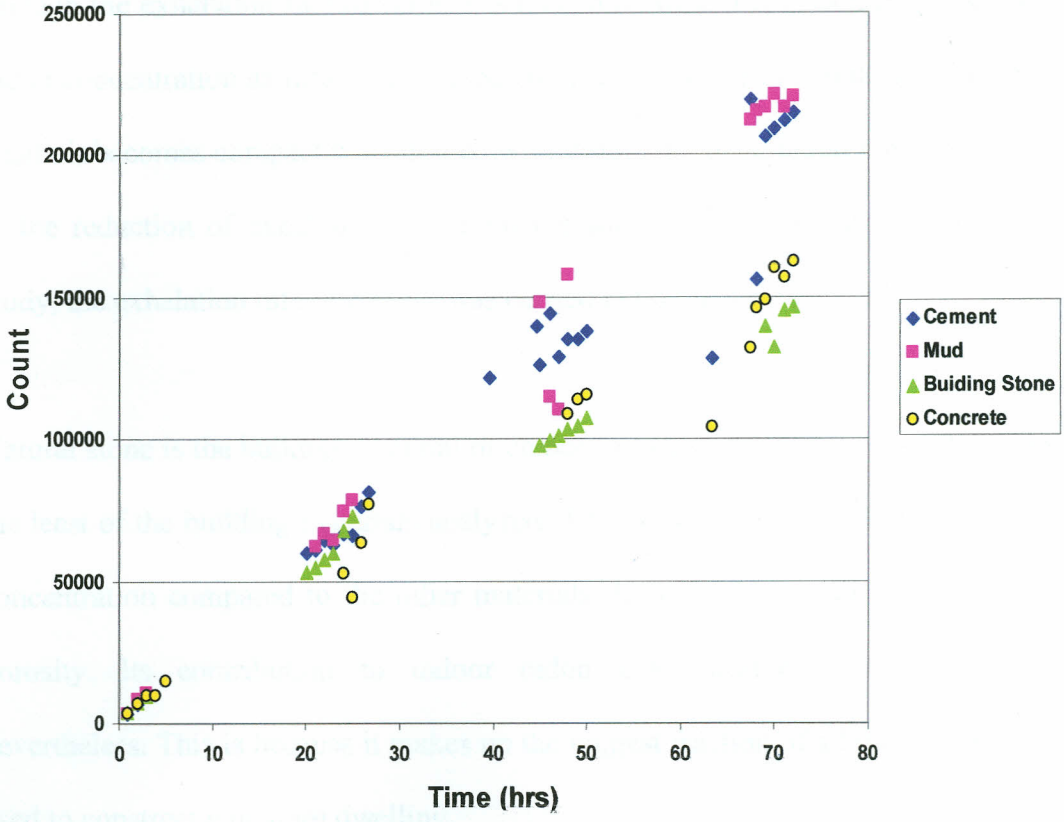


**Figure 5.5: $^{222}$Rn Exhalation Rates from Selected Building Materials**

The exhalation rate of the mud from the walls of the traditional huts was found to be the highest. The radium content in the mud was found to be very high. Again, mud is not compact. It has a very high porosity due to the fact that mostly its preparation is done manually. The high porosity allows for easy movement of radon gas from the solid matrix to the atmosphere. This high radon exhalation rate could have been the major contributor to indoor radon concentration in the model traditional huts. These huts were better ventilated when compared to the modern buildings, yet significant radon levels were reported.

Though the exhalation rate of cement is relatively high, it may contribute less to indoor radon concentration as little of it is used compared to other material like building stones. Again it becomes compact when mixed with water and the reduction in porosity may lead in the reduction of exhalation rate from the surface of the building. In this particular study, the exhalation rate of cement was carried out using raw cement.

Natural stone is the building material of choice in many urban areas. Its exhalation rate is the least of the building materials analyzed. This could be attributed to the lower radium concentration compared to the other materials. It is also more compact, hence reduced porosity. Its contribution to indoor radon concentration cannot be overlooked, nevertheless. This is because it makes up the biggest fraction of all the building materials used to construct a modern dwelling.

Concrete is made up of pieces of stone, sand and cement. During the curing of concrete, many tiny pores are left and this act as pathways through which radon moves. The exhalation rate is higher than that of natural stone though lower than cement. Concrete mostly makes the floor and the roof of most modern buildings, which are often airtight and therefore could contribute to significant amounts of radon to indoor air.

# CONCLUSION

From the research findings, it is evident that the level of ventilation (hence building design) does affect the radon concentrations as the basement room, which had the poorest ventilation reported the highest values, despite radium levels in its building materials and radon exhalation rates being lower. This is also evident in the Kikuyu and the Luo huts. The room where the canister was placed in the Luo hut had lower ventilation rate as compared to the Kikuyu hut. Considering that the two dwellings are similarly designed, the ventilation factor could have brought about the difference in radon concentrations.

Statistical analysis (ANOVA) shows that there was no significant change in radon concentration between (most) dwellings as compared to the difference within buildings. This means that factors other than the building design are responsible for fluctuations in radon concentration, and this could be due to the exhalation rates and radium levels in the building materials, as well as meteorological conditions.

The traditional huts remained open throughout the sampling period, yet, contrary to expectations, the indoor radon concentration was quite high. This is an indication that ventilation is not the only influential factor; the radon exhalation rate and the radium content are also important. The exhalation rates of the materials used in the traditional huts were higher than those used to construct both the classroom and the basement room. This is an indication that the nature of the building materials has an effect on indoor radon concentration.

The effects of the meteorological parameters were evident throughout the sampling period. The sinusoidal variation in radon concentration is one such effect. This could have resulted due to temporal variation in meteorological parameters such as moisture content in the soil and temperature.

The research findings indicated a significant radon concentration in the model traditional dwellings despite the fact that they were better ventilated as compared to the modern buildings. In normal circumstances, dwellers of such huts tend to keep them tightly shut regardless of the season for security reasons. The radon concentration would therefore be expected to be even higher. During the cold season, open fires are often lit in these huts and these could further lead to even higher radon concentrations due to the influence of pressure gradient.

## RECOMMENDATIONS

It is evident from the result of this research that indoor radon concentrations are high in some of the dwellings studied. Ventilation is still the prime factor, so it is advisable that dwellings are well ventilated to prevent build up of radon in indoor air. Some building materials can also contain high levels of radium; radon precursor, therefore building materials may be tested prior to construction. In areas where levels of radium is high, alternative building materials other than soil should be used, for example, building stones which have a lower exhalation rate.

The radon concentrations reported in this thesis are above the EPA recommended level of 148 $Bq/m^3$. Considering that more people now spend more times indoor, it is recommended that large-scale radon surveys should still be carried out to determine the prevalence of high indoor radon occurrence in Kenya.

## REFERENCES


1. Akerblom, G., Mjönes, L., Annanmäki, M., Magnusson, S., Strand, T., Ulbak, K. (2000). Naturally Occurring Radioactivity in the Nordic Countries – Recommendations. The Radiation Protection Authorities in Denmark, Finland, Iceland, Norway and Sweden ISBN 91-89230-00-0.
2. Anastasiou, T., Tsertos, H., Christofides, S. and Christodoulides, G. (2003). Indoor radon ($^{222}$Rn) concentration measurements in Cyprus using high-sensitivity portable detectors. *J. Envi. Radioactivity*, **68**: Pp159-169.
3. Bailey, M. R., (1994). The new ICRP model for the respiratory tract. *Radiation Protection Dosimetry* **53**: pp 107-114.
4. Baixerax, C., Erlandsson, B., Font, L., Johnson G. (2001). Radon emanation from soil samples. *Radiation Measurements,* **34:** pp 441.
5. Battaglia, A., Capra, D., Queirazza, G. and Sampaolo, A. (1990). Radon exhalation rate in building materials and fly ashes in Italy. *Proceedings of the 5th International Conference on Indoor Air Quality and Climate, Toronto, 29 July - 3 August*, **3:** pp.47-52.
6. Becker K., (2004). One century of radon therapy. *International Journal on Low Radiation,* **3:** Pp334-357
7. BEIR IV Report, (1988). Committee on the Biological Effects of Ionizing Radiation. National Research Council. Health risks of radon and other internally deposited alpha emitters: Washington (DC): National Academy Press.
8. BEIR VI report, (1999). Committee on the Biological Effects of Ionizing Radiation. National Research Council. Health Effects of Exposure to Radon. National academy Press, Washington, DC.
9. Conkwright, R. D. and Gast, R. A. (2005). Radon and Your Home. Division of Coastal and Estuarine Geology, Maryland Geological Survey, Baltimore.
10. Doi, M. and Kobayashi, S. (1994). Characterization of Japanese wooden houses with enhanced radon and thoron concentrations. *Health Physics* **66**(3): pp 274-282.
11. Dumont, R. S. and Figley D. A., (1988). Control of Radon in Houses. Canadian Building Digests: CBD-247.
12. El-Hussein, A., Mohammed, A. and Ahmed, A. A. (1998). A Study on Radon and Radon Progeny in Surface Air of El-Minia, Egypt. *Radiation Protection Dosimetry*, **78** (2): pp139-145.
13. EPA (1986). Radon reduction techniques for detached houses: technical guidance. EPA/625/5-86/019, United States Environmental Protection Agency, Office of Research and Development. Washington, D.C.
14. EPA (1990c). Toxicological profile for uranium. United States Environmental Protection Agency, US Department of Health and Human Services: TP-90-29. Washington D.C.

15. EPA (2001). Building radon out: A step-by-step guide on how to build radon-resistant homes. United States Environmental Protection Agency, Office of Air and Radiation: 402-K-01-002 Washington D.C.

16. EPA News Release (2005). International Effort to Reduce Radon Risk. Release date: 06/24/2005.

17. European Commission (1998). Scientific seminar on radiation protection in relation to radon: Directorate General, Environment, Nuclear Safety and Civil Protection.

18. European commission (2000). Risk assessment in relation to indoor air quality. European collaboration action. Urban air, indoor environment and human exposure. Environment and quality of life, report No. 22

19. Freidman, A. L., (2000). Indoor Radon Pollution at Bryn College. BIOL/ANTH/GEOL 397.

20. Garcia, R., Natale, G., Monnin, M., Seidel, Jean-Luk. (2000). Shock wave radon shock signals associated with the upsurge of T-P solitons in volcanic systems. *Journal of volcanology and geothermal research,* **96,** (1-2)**:** Pp15-24.

21. Gesell, T. F. (1983). Background atmospheric Rn-222 concentrations outdoors and indoors: a review. *Health Physics,* **45:** pp 289-302.

22. Graaf, E. R., Spoel, W. H., Meijer, R. J. (1998). Modelling of radon transport in porous media. Proc. 7th Tohwa University International symposium, Fukuoka, Japan, Oct. 23–25, 1997: pp E-218.

23. Greene, L. A. 2000. Reducing radon state by state. *Journal of Environmental Health,* **63** (2): Pp166.

24. Hafez, A. F., Bishara, A. A., Kotb, M. A. and Hussein, A. S. (2003). Regular radon activity concentration and effective dose measurements inside the great pyramid with passive nuclear track detectors. Health Physics, **85** (2): pp210-215.

25. Hashim, N. O. (2001). The Levels of Radionuclides and Trace Elements in Selected Kenyan Coastal Ecosystems. M.Sc. (Physics) Thesis. Kenyatta University. Nairobi, Kenya.

26. Hirning, H. J. (1992). Radon in North Dakota**.** NDSU Extension Service, North Dakota State University: AE-969 (Revised), 1992.

27. Iyengar, M. A. R. (1990). The Natural Distribution of Radium, In; The Environmental Behavior of Radium, Technical Report 310, **1:** Pp59 – 128.

28. Knoll, G., F. (1989). Radiation detection and measurement (second edition). John Wiley and sons inc: Pp250.

29. Krewiski, D. S., Rai, N. Z., Hopke, P. K. (1999). Characteristics of uncertainties and variability in residential cancer risks. *Annals of the New York Academy of science,* **895**: pp 245-272.

30. LaFavore, M. (1987). Radon, the Invisible Threat. Pennsylvania: Rodale Press. pp 257.

31. Maged, A. F. and Ashraf, F. A. (2005). Radon Exhalation Rate of Some Building Materials Used in Egypt. *Environmental Geochemistry and Health*, **27** (5): pp. 485-489.

32. Mahmoud K, (2004). Assessment of radon-222 concentrations in buildings, building materials, water and soil in Jordan. Physics Department, Yarmouk University, Irbid 211-63, Jordan.

33. Maina D. M., Kinyua A. M., Nderitu S. K., Agola, J .O. and Mangala, M. J., (2004). Indoor Radon Levels in Coastal and Rift Valley Regions of Kenya. IAEA-CN-91/56: pp 401-404.

34. MARSSIM, Revision 1, (August, 2000): Field measurements methods and instrumentations: pp 632-635.

35. Martino S, C., Sabbarese, G., Monetti (1998). Radon emanation and exhalation rates from soils measured with an electrostatic collector. *Applied Radiation and Isotopes*, **49** (4): pp 407.

36. Michel van der Pal (2003). Radon Transport in Autoclaved Aerated Concrete. Ph.D. Thesis: Eindhoven: Technische Universiteit Eindhoven.

37. Mohanty, A. K., Sengupta, D., Das, S. K., Vijayan, V. and Saha S. K. (2003). Natural radioactivity in the newly discovered high background radiation area on the eastern coast of Orissa, India. *Radiation Measurements,* **38**: pp153-165.

38. Mustapha, A. O. (1999). Assessment of human exposure to natural sources of radiation in Kenya. Ph.D. Thesis. University of Nairobi, Kenya.

39. Nero, A. V., Nazaroff, W. W., (1984). Characterizing the Source of Radon Indoors. *Radiation Protection Dosimetry,* **7**: pp 23-39.

40. Ng, C. Y., Leung, J. K. C. and Tso, M. Y. W. (1995). Modeling exposure to naturally occurring radionuclides in building materials, *Radiation Protection Dosimetry*, **59** (1): Pp43 – 48.

41. Olsson M. and Tengström J. (2004). RADON: Presence and Remedial Measures in Europe and the USA: Thesis for the degree of Master of Science: Chalmers University of Technology Göteborg, Sweden.

42. Orlando, P., Trenta R., Bruno M., Orlando C., Ratti A., Ferrari S. and Piardi S., (2004). A study about Remedial Measures to Reduce Radon Concentration in an Experimental Building. Journal of Environmental Radioactivity **73** (3): Pp257-266.

43. Planinic, J., Radolic, V., Lazanin, Z. (2001). Temporal variations of radon in soil related to earthquakes. *Applied radiation and isotopes*, **55** (2): pp 267-272.

44. Price, J.G., Rigby, J.G., Christensen, L., Hess, R., LaPointe, D.D., Ramelli, A.R., Desilets, M., HoPper, R.D., Kluesner, T. and Marshall, S. (1994. Radon in outdoor air in Nevada, *Health Physics,* **66**: pp 433-438.

45. Richon, P., Sabroux, J. C., Halbwachs, M., Vandemeulebrouck, J., Poussielgue, J., Tabbagh, N. and Punongbayan R. (2003). Radon anomaly in the soil of Taal volcano,

the Philippines: A likely precursor of the M 7.1 Mindoro earthquake (1994) *geophysical research letters*, **30** (9), 1481, doi: 10.1029/2003GL016902: pp 341-344

46. Sakashita, T., Doi, M. and Nakamura, Y. (2004). A case study of radon-222 transport from continental North-east Asia to the Japanese Islands in winter by numerical analysis. *Journal of Environmental Radioactivity*, **72** (3): pp 245 – 257.

47. Samet M. J. and Eraddze G. R. (2000). Radon and Lung cancer: Taking Stock at the Millenium. Environmental and Occupational Lung Diseases.

48. Sciocchetti, G. (1992). Indoor radon and thoron survey in high radioactivity areas of Italy. *Radiation protection dosimetry*, **45** (1/4): pp 509–513.

49. Sengupta, D., Ghosh, A. and Mamtani, M. A. (2005). Radioactivity studies along fracture zones in areas around Galudih, East Singhbhum, Jharkhand, India. *Applied Radiation and Isotopes,* **63**: pp 409-414

50. Sengupta, D., Kumar, R., Singh, A. K. and Prasad, R. (2001). Radon exhalation and radiometric prospecting on rocks associated with Cu-U mineralizations in the Singhbhum shear zone, Bihar. *Applied Radiation and Isotopes,* **55**: pp 889-894.

51. Shweikani, R. T. G., Giaddui, S. A., Durrani (1995). The effect of soil parameters on the radon concentration values in the environment. *Radiation Measurements,* **5: (**1–4), pp 581.

52. Sun, K., Guo, Q. and Zhuo, W. (2004). Feasibility for mapping radon exhalation rate from soil in china. *Nuclear Science and Technology*, **41**: pp 86-90.

53. Synnott, H., Hanley, O., Fenton, D. and Colgan, P. A. (2006). Radon in Irish schools: the results of a national survey. *Journal Of Radiological Protection,* **26:** pp85–96

54. Tyson, J.L., Fairey, P.W. and Withers, C.R. (1993). Elevated radon levels in ambient air; Proceedings of the 6th International Conference on Indoor Air Quality and Climate, Helsinki, Finland, July 4-8,1993, **4:** pp 443-448.

55. UI (University of Iowa) Health Care News (2005). Study Shows Link Between Residential Radon Exposure and Lung Cancer. Release date: Week of March 21, 2005.

56. UNSCEAR (1977). *Sources and Effects of Ionizing Radiation.* United Nations Scientific Committee on the Effects of Atomic Radiation, 1977 Report to the general assembly, United Nations, New York.

57. UNSCEAR (1982). *Sources of ionizing radiation.* United Nations Scientific Committee on Effects of Atomic Radiation, 1982 Report to the General Assembly, United Nations, New York.

58. UNSCEAR (1988). *Sources, Effects And Risks Of Ionizing Radiation.* United Nations Scientific Committee on Effects of Atomic Radiation, 1998 Report, United Nations, New York.

59. UNSCEAR (1993). *Sources of ionizing radiation.* United Nations Scientific committee on Effects of Atomic Radiation, 1993 Report, United Nations, New York.

60. UNSCEAR (2000); United Nations Scientific Committee on the Effects of Atomic Radiation. *Sources and Effects of Ionizing Radiation. UNSCEAR 2000 Report to the General Assembly, with Scientific Annexes.Vol I: Sources*. New York: United Nations, 2000.

61. Viera, A. J. (2000). Radon and lung cancer. *American family physician,* **65** (5): pp 550.


**Figure A1: Traditional house of Kikuyu community**

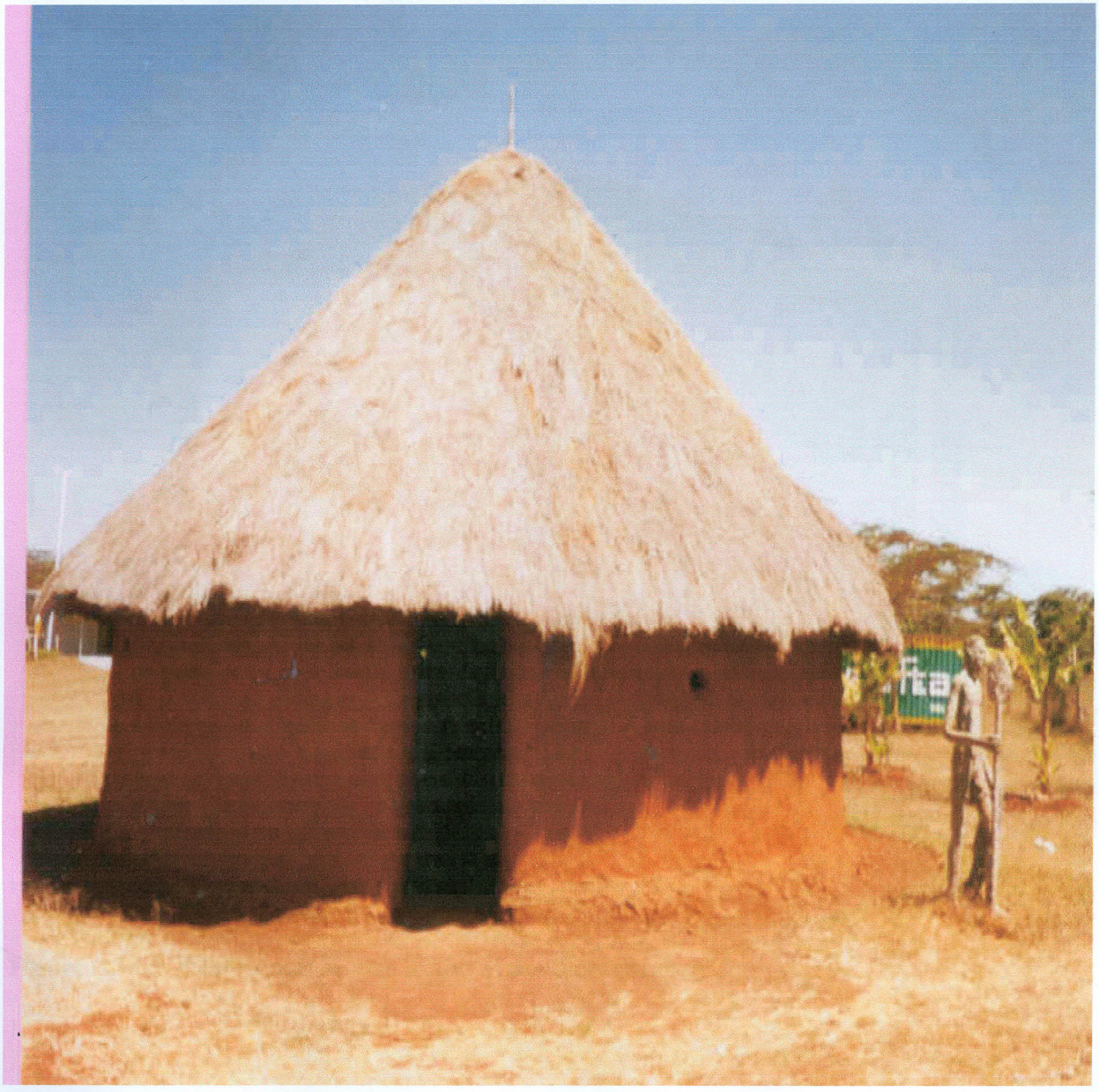

**Figure A2: Traditional house of Luo community**

**Figure A3: Traditional House of the Maasai community**

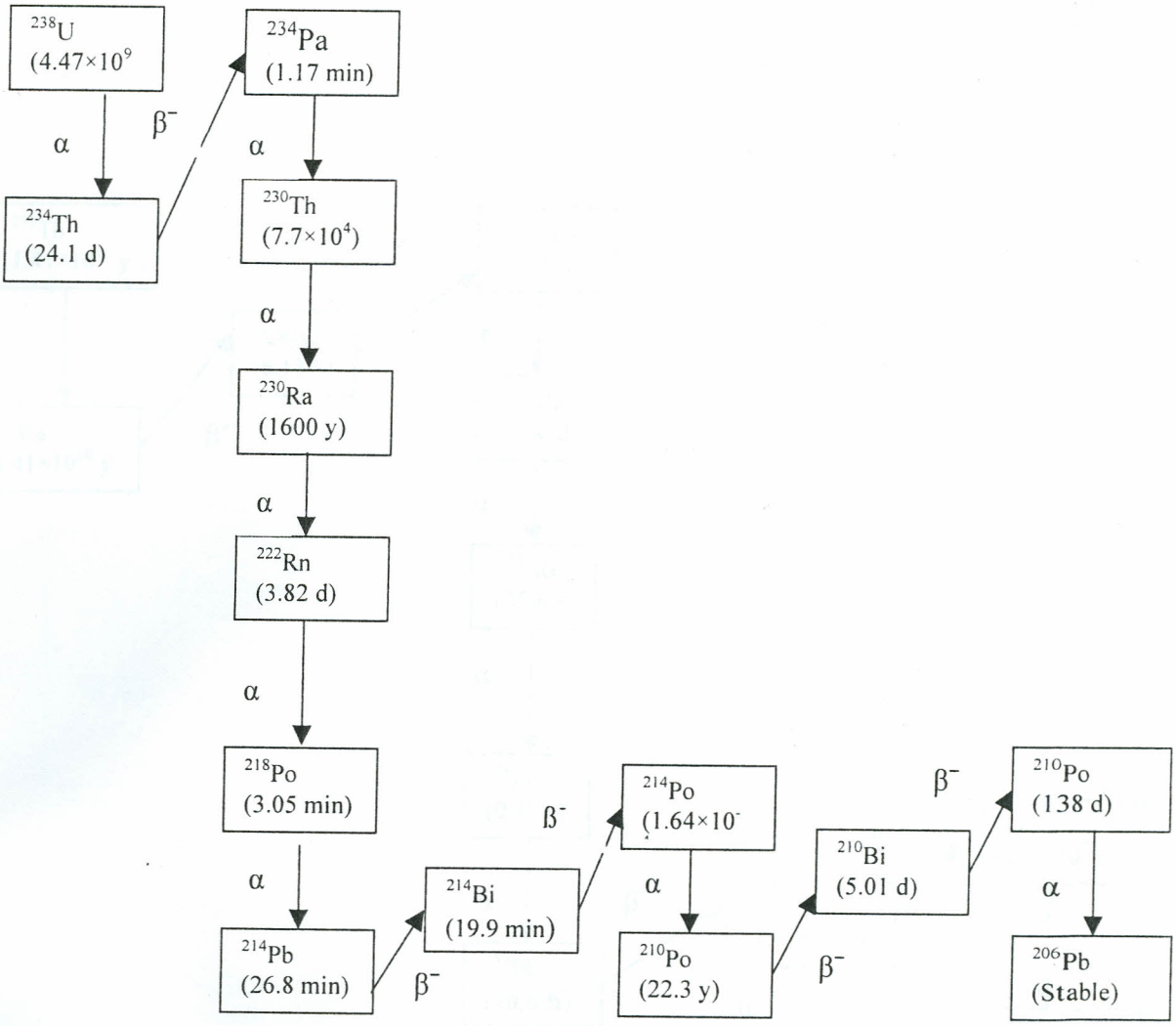


**Figure A5: $^{238}$U decay series**

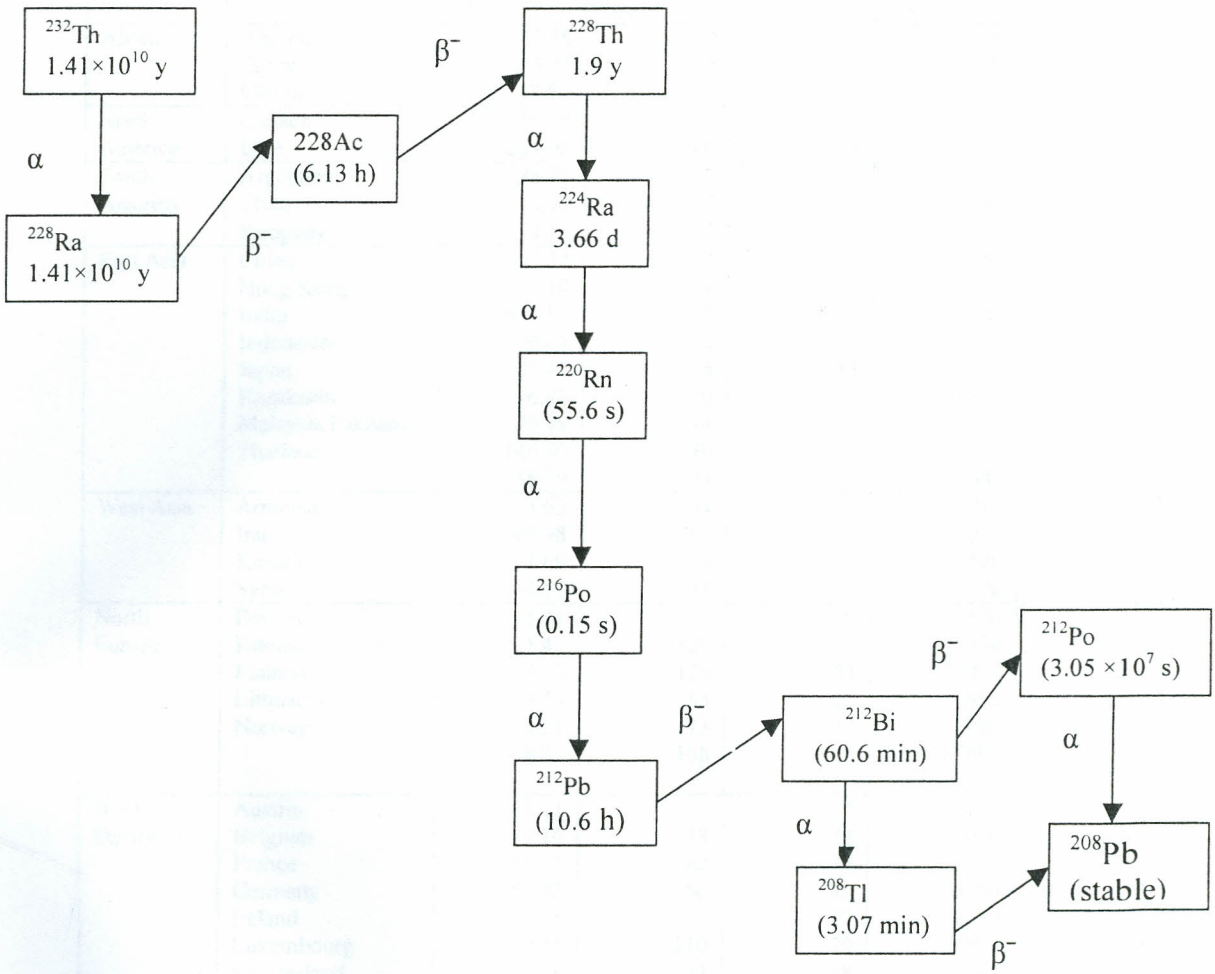


**Figure A6: $^{232}Th$ decay series**

**Table A1: $^{222}$Rn Concentration in Dwellings Determined in Indoor Surveys (UNSCEAR 2000)**

| *Region* | *Country* | *Population in 1996 ($10^6$)* | *Radon concentration ($Bq/m^3$)* | | | *Geometric standard deviation* |
|---|---|---|---|---|---|---|
| | | | *Arithmetic mean* | *Geometric mean* | Maximum value | |
| Africa | Algeria | 28.78 | 30 | | 140 | |
| | Egypt | 63.27 | 9 | | 24 | |
| | Ghana | 17.83 | | | 340 | |
| North America | Canada | 29.68 | 34 | 14 | 1720 | 3.6 |
| | USA | 269.00 | 46 | 25 | | 3.1 |
| South America | Argentina | 35.22 | 37 | 26 | 211 | 2.2 |
| | Chile | 14.42 | 25 | | 86 | |
| | Paraguay | 4.96 | 28 | | 51 | |
| East Asia | China | 1232 | 24 | 20 | 380 | 2.2 |
| | Hong Kong | 6.19 | 41 | | 140 | |
| | India | 944.60 | 57 | 42 | 210 | 2.2 |
| | Indonesia | 200.45 | 12 | | 120 | |
| | Japan | 125.40 | 16 | 13 | 310 | 1.8 |
| | Kazaktsan | 16.82 | 10 | | 6000 | |
| | Malaysia Pakistan | 20.58 | 14 | | 20 | |
| | Thailand | 140.00 | 30 | | 83 | |
| | | 58.70 | 23 | 16 | 480 | 1.2 |
| West Asia | Armenia | 3.63 | 104 | | 216 | 1.3 |
| | Iran | 69.98 | 82 | | 3070 | |
| | Kuwait | 1.69 | 14 | | 120 | |
| | Syria | 14.57 | 44 | 6 | 20 | |
| North Europe | Denmark | 5.24 | 53 | 29 | 600 | 2.2 |
| | Estonia | 1.47 | 120 | 92 | 1390 | |
| | Finland | 5.13 | 120 | 84 | 20000 | 2.1 |
| | Lithuania | 3.73 | 55 | 22 | 1860 | |
| | Norway | 4.35 | 73 | 40 | 50000 | |
| | | 8.83 | 108 | 56 | 85000 | |
| West Europe | Austria | 8.11 | | 15 | 190 | |
| | Belgium | 10.16 | 48 | 38 | 12000 | 2.0 |
| | France | 58.33 | 62 | 41 | 4690 | 2.7 |
| | Germany | 81.92 | 50 | 40 | >10000 | 1.9 |
| | Ireland | 3.55 | | 37 | 1700 | |
| | Luxembourg | 0.41 | 110 | 70 | 2500 | 2.0 |
| | Switzerland | 15.58 | 23 | 18 | 380 | 1.6 |
| | UK | 7.22 | 70 | 50 | 10000 | |
| | | 58.14 | 20 | | 10000 | |
| Eastern Europe | Bulgaria | 8.47 | | 22 | 250 | |
| | Czech republic | 10.25 | 140 | | 20000 | |
| | Hungary | 10.05 | 107 | 82 | 1990 | 2.7 |
| | Poland | 38.60 | 41 | 32 | 432 | 2.0 |
| | Romania | 22.66 | 45 | | 1025 | |
| | Slovakia | 5.35 | 87 | | 3750 | |
| Southern Europe | Albania | 3.40 | 120 | 105 | 270 | 2.0 |
| | Croatia | 4.50 | 35 | 32 | 92 | |
| | Cyprus | 0.76 | 7 | 7 | 78 | 2.6 |
| | Greece | 10.49 | 73 | 52 | 490 | |
| | Italy | 57.23 | 75 | 57 | 1040 | 2.0 |
| | Portugal | 9.81 | 62 | 45 | 200 | 2.2 |
| | Slovenia | 1.92 | 87 | 60 | 1330 | 2.2 |
| | Spain | 39.67 | 86 | 42 | 15400 | 3.7 |
| Oceania | Australia | 18.06 | 11 | 8 | 420 | 2.1 |
| | New Zealand | 3.60 | 20 | 18 | 90 | |
| Median | | | 46 | 37 | 480 | 2.2 |
| population-weighed average | | | 39 | 30 | 1200 | 2.3 |